JPET Fast Forward. Published on July 29, 2016 as DOI: 10.1124/jpet.116.235044
This article has not been copyedited and formatted. The final version may differ from this version.

Regulation of UGT2B expression and activity by miR-216b-5p in liver cancer cell lines

Douglas F. Dluzen, Aimee K. Sutliff, Gang Chen, Christy Watson, Faoud T. Ishmael, and Philip Lazarus

National Institute on Aging, NIH Baltimore, MD (D.F.D); Department of Pulmonary Medicine, Penn State University College of Medicine, Hershey, PA (F.T.I); Department of Pharmaceutical Sciences, Washington State University College of Pharmacy, Spokane, WA (A.K.S., G.C., C.W., P.L.)

Downloaded from jpet.aspetjournals.org at ASPET Journals on April 19, 2024

JPET Fast Forward. Published on July 29, 2016 as DOI: 10.1124/jpet.116.235044
This article has not been copyedited and formatted. The final version may differ from this version.

Running title: Regulation of UGT2B expression and activity by miR-216b-5p

Corresponding author: Philip Lazarus, Ph.D., Department of Pharmaceutical Sciences, Washington State University College of Pharmacy, PO Box 1495, Spokane, WA, 99210; Phone: 509-358-7947; Fax: 509-358-7967

Email: phil.lazarus@wsu.edu

Document Statistics:

Text pages: 34

Tables: 1

Figures: 6

References: 42

Abstract words: 244

Introduction words: 547 (not including citations)

Discussion words: 1208 (not including citations)

Abbreviations: mass spectrometry (MS); microRNA (miRNA); quantitative reverse-transcription polymerase chain reaction (qRT-PCR); single nucleotide polymorphism (SNP); site-directed mutagenesis (SDM); UDP-glucuronosyltransferase (UGT); ultra-pressure liquid chromatography (UPLC); untranslated region (UTR); Uridine diphosphate glucuronic acid (UDPGA)

Recommended section assignment: Metabolism, Transport, and Pharmacogenomics

Downloaded from jpet.aspetjournals.org at ASPET Journals on April 19, 2024

JPET Fast Forward. Published on July 29, 2016 as DOI: 10.1124/jpet.116.235044
This article has not been copyedited and formatted. The final version may differ from this version.

Abstract

The UDP-glucuronosyltransferase (UGT) 2B enzymes are important in the detoxification of a variety of endogenous and exogenous compounds including many hormones, drugs and carcinogens. Identifying novel mechanisms governing their expression is important in understanding patient-specific response to drugs and cancer risk factors. *In silico* prediction algorithm programs were utilized to screen for microRNAs (miRNA) as potential regulators of UGT2B enzymes with miR-216b-5p identified as a potential candidate. Luciferase data suggested the presence of a functional miR-216b-5p binding motif within the 3′ untranslated regions of UGTs 2B7, 2B4 and 2B10. Over-expression of miR-216b-5p mimic significantly repressed UGT2B7 (P<0.001) and UGT2B10 (P=0.0018) mRNA levels in HuH-7 cells, and UGT2B4 (P<0.001) and UGT2B10 (P=0.018) mRNA in Hep3B cells. UGT2B7 protein levels were repressed in both HuH-7 and Hep3B cells in the presence of increasing miR-216b-5p concentrations, corresponding with significant (P<0.001 and P=0.011, respectively) decreases in glucuronidation activity against the UGT2B7-specific substrate, epirubicin. Inhibition of endogenous miR-216b-5p levels significantly increased UGT2B7 mRNA levels in HuH-7 (P=0.0205) and Hep3B (P=0.0068) cells, and increased epirubicin glucuronidation by 85% (P=0.057) and 50% (P=0.012) for HuH-7 and Hep3B cells, respectively. UGT2B4 activity against codeine and UGT2B10 activity against nicotine were significantly decreased in both HuH-7 and Hep3B cells (P<0.001 and P=0.0048, and P=0.017 and P=0.043, respectively) after over-expression of miR-216b-5p mimic. This is the first evidence that miRNAs regulate UGTs 2B7, 2B4 and 2B10 expression and that miR-216b-5p regulation of UGT2B proteins may be important in regulating the metabolism of UGT2B substrates.

Downloaded from jpet.aspetjournals.org at ASPET Journals on April 19, 2024

JPET Fast Forward. Published on July 29, 2016 as DOI: 10.1124/jpet.116.235044
This article has not been copyedited and formatted. The final version may differ from this version.

Introduction

The UGT2B gene subfamily is involved in the metabolic clearance of numerous endogenous compounds including bile acids and steroid hormones, as well as exogenous agents including a variety of carcinogens and drugs (Stingl et al.). UGT2B enzymes are well-expressed in the liver (Ohno and Nakajin, 2009) and identifying novel mechanisms of their regulation may provide insight into UGT2B enzymatic activity and overall metabolic response in humans.

The UGT2B gene family consists of seven isoforms: UGTs 2B4, 2B7, 2B10, 2B11, 2B15, 2B17, and 2B28 (Mackenzie et al., 2005). The UGT2B genes contain six coding exons with unique, individual promoters and individual 3′ untranslated regions (UTRs) (Mackenzie et al., 2005; Mackenzie et al., 2010). Given that the UGT2B gene subfamily exhibits >70% DNA sequence homology with one another (Riedy et al., 2000; Guillemette et al., 2010), they appear to have evolutionarily arisen through successive rounds of gene duplication and replication slippage. All UGT2B isoforms, excluding UGT2B28, are well-expressed in the liver in addition to other extra-hepatic tissues involved in metabolism including stomach, colon, small intestine and kidney (Nakamura et al., 2008; Ohno and Nakajin, 2009; Jones and Lazarus, 2014). In addition, several UGT2B isoforms are highly expressed in extra-hepatic tissues locally influenced by UGT2B substrates. For instance, UGT2B15 and UGT2B17 metabolize multiple sex steroid hormones, including dihydrotestosterone, androsterone, and epiestradiol (Chouinard et al., 2007; Itaaho et al., 2008), and exhibit high expression in steroidogenic tissues including breast, prostate, ovaries, uterus, and testes (Nakamura et al., 2008).

While the levels of combined hepatic mRNA expression of the UGT2B gene family is close to 70% of total hepatic UGT mRNA abundance, there is also a high degree of variability in

Downloaded from jpet.aspetjournals.org at ASPET Journals on April 19, 2024

JPET Fast Forward. Published on July 29, 2016 as DOI: 10.1124/jpet.116.235044
This article has not been copyedited and formatted. The final version may differ from this version.

the hepatic expression of all UGT2B isoforms (Izukawa et al., 2009). UGT2B7 protein levels can vary >4-fold (Izukawa et al., 2009; Sato et al., 2012) and there is no correlation between UGT2B7 mRNA and UGT2B7 protein levels within individual human liver tissue samples (Izukawa et al., 2009; Ohtsuki et al., 2012). A potential mechanism for regulating the expression of UGT2B7 and other UGT2B genes is by microRNAs (miRNAs). miRNA are single-stranded RNAs of approximately 22 nucleotides in length that, when coupled with the RNA-induced silencing complex (RISC), bind to target mRNA 3′ UTRs and inhibit protein translation, thereby reducing protein expression (Bartel, 2009; Carthew and Sontheimer, 2009). miRNA can also decrease target mRNA levels, but this effect is dependent on the concentrations of both the target mRNA and miRNA genes (Baek et al., 2008; Guo et al., 2010; Mukherji et al., 2011). Due to their imperfect binding, miRNA are highly promiscuous and can regulate several different genes at a given time. Reciprocally, many mRNAs can be targeted by several different miRNA at the same time (Brennecke et al., 2005; Brodersen and Voinnet, 2009). miRNAs are also involved in the regulation of multiple members of a single pathway, including upstream transcriptional regulators, and this complexity contributes to their role as fine-tuners of protein expression. For example, miR-27b regulates the expression of CYP3A4 in human pancreatic cancer cells and also regulates the expression of the vitamin D receptor (VDR) - an upstream transcriptional inducer of CYP3A4 (Pan et al., 2009).

Previous work in our laboratory identified miR-491-3p as a novel miRNA regulator of UGT1A gene expression (Dluzen et al., 2014). miR-491-3p expression levels were shown to be inversely correlated with UGT1A3 and UGT1A6 mRNA levels in normal human liver and contributed to observed inter-individual variability of UGT1A gene expression (Dluzen et al., 2014). Recent studies have demonstrated that miR-376c exhibits an inverse expression level with the androgen-metabolizing UGTs 2B15 and 2B17 in prostate cancer cells (Wijayakumara et al., 2015). The opposite relationship between miR-376c and UGT2B15/UGT2B17 expression

Downloaded from jpet.aspetjournals.org at ASPET Journals on April 19, 2024

JPET Fast Forward. Published on July 29, 2016 as DOI: 10.1124/jpet.116.235044
This article has not been copyedited and formatted. The final version may differ from this version.

was shown in healthy prostate tissue, suggesting that low expression of miR-376c may contribute to prostate cancer development in androgen-dependent tumors by dysregulation of androgen signaling (Wijayakumara et al., 2015; Margaillan et al., 2016).

In the present study, we provide evidence that miR-216b-5p regulates the expression of several UGT2B genes including UGTs 2B7, 2B4 and 2B10.

Downloaded from jpet.aspetjournals.org at ASPET Journals on April 19, 2024

JPET Fast Forward. Published on July 29, 2016 as DOI: 10.1124/jpet.116.235044
This article has not been copyedited and formatted. The final version may differ from this version.

Materials and Methods

Chemicals and Reagents. The pGL3-Promoter luciferase and pRL-TK renilla plasmids were obtained from Promega (Madison, WI). All synthesized DNA oligonucleotides used for 3′ UTR amplification, site-directed mutagenesis (SDM), and PCR analysis were from Integrated DNA Technologies, Inc (Coralville, IA) or Life Technologies (Carlsbad, CA). Lipofectamine 2000 transfection reagent was from Life Technologies. miRVana miRNA miR-216b-5p mimic (#MC12302), miRVana negative control mimic #1 (#4464058), miRVana miRNA miR-216b-5p inhibitor (#12302), and negative control inhibitor #1 (#4464076) were purchased from Ambion (Austin, TX). Codeine and (-)-nicotine, uridine 5′-diphosphoglucuronic acid (UDPGA), alamethicin, and bovine serum albumin (BSA) were from Sigma-Aldrich (St. Louis, MO). Epirubicin hydrochloride was purchased from Toronto Research Chemicals (Toronto, ON, Canada). Rabbit anti-UGT2B7 and anti-β-actin antibodies were from BD Biosciences (San Jose, CA) and Cell Signaling Technologies (Danvers, MA), respectively. All other chemicals were purchased from Fisher Scientific (Pittsburg, PA) unless specified otherwise.

Cells and Culture Conditions. Human embryonic kidney cell line 293 (HEK293), human liver adenocarcinoma cell line SK-HEP-1, human hepatocellular carcinoma cell lines HepG2 and Hep3B, colon adenocarcinoma cell line Caco-2, human breast adenocarcinoma cell line MCF-7, and human lung carcinoma cell line A-549 were purchased from the American Type Culture Collection (ATCC, Manassas, VA). The human hepatocellular carcinoma cell line HuH-7 was a kind gift from Dr. Jianming Hu (Penn State University, Hershey, PA). Hep3B, HEK293, A-549 and HuH-7 cells were cultured in DMEM (Gibco, Carlsbad, CA) supplemented with 10% FBS (Atlanta Biologicals, Lawrenceville, GA) and 1% penicillin/streptomycin (Gibco). SK-HEP-1 cells were cultured in RPMI 1640 (Gibco) supplemented with 10% FBS, 1%

Downloaded from jpet.aspetjournals.org at ASPET Journals on April 19, 2024

JPET Fast Forward. Published on July 29, 2016 as DOI: 10.1124/jpet.116.235044
This article has not been copyedited and formatted. The final version may differ from this version.

penicillin/streptomycin, and 1% Non-Essential Amino Acids (NEAA). HepG2 and Caco-2 cells were cultured in DMEM supplemented with 10% FBS, 1% penicillin/streptomycin, and 1% NEAA (Lonza, Basel, Switzerland). MCF-7 cells were cultured in RPMI 1640 supplemented with 10% FBS and 1% penicillin/streptomycin. All cells were grown and maintained in 5% CO_2 at 37°C.

Tissues and miRNA Isolation. Pathologically normal colon and endometrium specimens (n=5 each) were obtained from the tissue bank at Pennsylvania State University College of Medicine (Hershey, PA). Pathologically normal liver specimens (n=5) and their matching total RNA were obtained from the H. Lee Moffitt Cancer Center Tissue Procurement Facility (Tampa, FL). All protocols involving the collection and analysis of tissue specimens from these tissue banks were approved by the Institutional Review Boards at their respective institutions and were in accordance with assurances filed with and approved by the United States Department of Health and Human Services. Normal jejunum tissue specimens were purchased from the Sun Health Research Institute (Sun City, AZ). All tissue samples were isolated and frozen at -70°C within 3 h post-surgery. Colon, liver, jejunum, endometrium and cell line total RNA was extracted using the RNeasy Mini Kit (Qiagen, Hilden, Germany). Total RNA samples from cell lines were subject to on-column DNAse digestion during RNA purification (Qiagen). Pooled breast total RNA was purchased from the Biochain Institute (Hayward, CA) while lung, pancreas, larynx, trachea, and kidney RNA was purchased from Clontech (Mountain View, CA) or Agilent (Santa Clara, CA). Small RNA (<200 nt) containing the miRNA fraction was isolated and purified from total RNA using the mirVana miRNA Isolation Kit (Ambion). RNA concentrations were determined using a Nanodrop ND-1000 spectrophotometer (Thermo Scientific) and were eluted and stored as aliquots in RNase-, DNAse-free water in a -80°C freezer.

miRNA Binding Site Predictions. The 3′ UTR sequences of UGT2B enzymes were obtained from the NCBI Reference Sequence Database. miRNA binding site predictions were

Downloaded from jpet.aspetjournals.org at ASPET Journals on April 19, 2024

JPET Fast Forward. Published on July 29, 2016 as DOI: 10.1124/jpet.116.235044
This article has not been copyedited and formatted. The final version may differ from this version.

obtained using, (i) TargetScan (Lewis et al., 2005), scored with the Total Context+ score as described in Garcia et. al (Garcia et al., 2011), and (ii) miRanda, algorithm v3.0 (Betel et al., 2008) with the following parameters: Gap Open Penalty, -8.00; Gap Extend, -2.00; Score Threshold, 50.00; Energy Threshold, -20.00 kcal/mol; Scaling Parameter, 4.00.

Real-Time Quantitative PCR. cDNAs were synthesized from total RNA using the SuperScript First-Strand Synthesis Kit (Invitrogen, Carlsbad, CA). miRNA cDNAs were synthesized using the Taqman MicroRNA Reverse Transcription Kit (Ambion). Taqman gene expression assays (Applied Biosystems, Carlsbad, CA) were used to quantify UGT2B7 (Hs_02556232_s1), UGT2B4 (Hs_02383831_s1), UGT2B10 (Hs_02556282_s1), UGT2B11 (Hs_01894900_gH), UGT2B15 (Hs_00870076_s1), UGT2B17 (Hs_00854486_sH), and Ribosomal protein, large, P0 (RPLP0) (Hs99999902_m1). Taqman microRNA assays (Ambion) were used to quantify miR-216b-5p (Cat. # 4427975, ID #002326) and RNU6B endogenous control (Cat #4427975, ID #001093) in all cell lines and tissue samples. PCR reactions were performed in 10 µL reactions in 384-well plates using an ABI 7900HT Sequence Detection System, with incubations performed at 50°C for 2 minutes, 95°C for 10 minutes, followed by 40 cycles of 95°C for 15 sec, 60°C for 1 minute. Reactions included 2x Universal PCR Master Mix (Applied Biosystems), Taqman gene expression primers or Taqman miRNA primers, and corresponding cDNA, following the manufacturer's protocol. Each plate included a no DNA negative control and all reactions were performed in quadruplicate. Gene expression was compared to an endogenous, internal control (RPLP0 for mRNA or RNU6B for miRNA) using the $2^{-\Delta\Delta C_T}$ method (Livak and Schmittgen, 2001). C_T values were determined using the SDS 2.4 software (Applied Biosystems) and amplification C_T values higher than 40 cycles were designated as below the limit of detection (B.L.D.).

Construction of Reporter Plasmids. The luciferase reporter plasmids used in this study were constructed by inserting the 3′ UTRs of UGTs 2B7, 2B4 and 2B10 into the *XbaI*

Downloaded from jpet.aspetjournals.org at ASPET Journals on April 19, 2024

JPET Fast Forward. Published on July 29, 2016 as DOI: 10.1124/jpet.116.235044
This article has not been copyedited and formatted. The final version may differ from this version.

restriction site downstream of the luciferase reporter gene in the pGL3-Promoter vector. Briefly, primers containing a *XbaI* restriction enzyme site (see Table 1) were used to amplify UGT2B 3′ UTRs using genomic DNA isolated from the HEK293 cell line. Two sets of primers were used to amplify the 3′ UTR of UGT2B7 because of sequence similarities with other UGT2B genes: UGT2B7 “outer primers” amplified the UGT2B7 3′ UTR containing 5′ upstream exon and 3′ downstream intergenic DNA sequences, and UGT2B7 “inner primers” amplified the UGT2B7 3′ UTR from the resulting PCR product from the “outer primers” amplification. Each amplified region was cloned into the *XbaI* restriction site of the pGL3-Promoter vector. The miR-216b-5p seed deletion plasmids were created by performing site directed mutagenesis (SDM) using the QuikChange II Site Directed Mutagenesis Kit (Agilent, Santa Clara, CA) and the forward and reverse mutagenesis primers listed in Table 1. A UGT2B10 vector containing the A>G SNP at position 155 of the UGT2B10 3′ UTR was created by SDM with the pGL3-Promoter vector containing the ‘wild-type’ (wt) UGT2B10 3′ UTR sequence as template and primers whose sequences are also listed in Table 1. Nucleotide sequences of all plasmids used in this study were confirmed by DNA sequencing analysis performed at the Pennsylvania State University Nucleic Acids Core Facility (State College, PA).

Luciferase Assays. The pGL3-Promoter vector cloned with each 3′ UTR was co-transfected with the pRL-TK renilla control vector and miRVana miRNA mimics into HEK293 cells. The day before transfection, HEK293 cells were seeded onto 24-well plates at 50,000 cells/well, and after 24 h were co-transfected with 380 ng of UGT2B 3′ UTR-containing pGL3 plasmid and 20 ng of the pRL-TK plasmid together with either scrambled miRNA control or various concentrations of miRNA mimic, using Lipofectamine 2000 transfection reagent according to manufacturer’s protocol. Transfected HEK293 cells were harvested 24 h post-transfection using passive lysis buffer and luciferase activity was measured with a luminometer

Downloaded from jpet.aspetjournals.org at ASPET Journals on April 19, 2024

JPET Fast Forward. Published on July 29, 2016 as DOI: 10.1124/jpet.116.235044
This article has not been copyedited and formatted. The final version may differ from this version.

(Bio-tek Synergy HT, Winooski, VT) using the Dual-Luciferase Reporter Assay System (Promega, Madison, WI). All luciferase assay experiments were performed in triplicate.

Western Blot Analysis. UGT2B7 and β-actin protein levels were determined via immunoblotting. For each Western blot, 15 µg of cellular homogenate and loading buffer were heated at 90°C for 10 min. Samples were run at 90 V on a 12% acrylamide gel and transferred to a polyvinylidene diflouride (PVDF) membrane for 2 h at 33 V. PVDF membranes were blocked in 5% milk in Tris-buffered Saline with Tween 20 (TBS-T) for 1 h, probed with primary antibody (1:1000 dilution) overnight at 4°C, washed 3x, and incubated with the appropriate secondary antibody (1:5000 dilution). Protein bands were visualized using the Amersham ECL Prime Western Blotting Detection Reagent (GE Healthcare, Pittsburgh, PA) and Hyoblot CL autoradiography film (Denville Scientific, Metuchen, NJ). UGT2B7 protein blots were stripped and re-probed for β-actin, which served as the loading control.

Glucuronidation Assays. Cell homogenates for glucuronidation activity assays were harvested 48 h post transfection. HuH-7 or Hep3B cells were transfected with either scrambled miRNA controls, various concentrations of miR-216b-5p mimic, or 100 nM miR-216b-5p inhibitor using 30-50 uL Lipofectamine 2000 in 10 cm dishes, according to the manufacturer's protocol, as previously described (Dellinger et al., 2007). Collected cell pellets were subjected to three freeze-thaw cycles and three 10-sec pulses using a hand-held Bio-Vortexer (Biospec, Bartlesville, OK) prior to storage at -80°C. Protein concentration was quantified using the BCA Protein Assay Kit (Pierce Chemical, Rockford, IL) and measured using either an Appliskan Luminometor with SkanIT Software v2.3 (Thermo Scientific) or the Synergy Neo and Gen5 Data Analysis Software (BioTek).

The glucuronidation assays using homogenates from HuH-7 and Hep3B cells were performed as described previously (Sun et al., 2007; Sun et al., 2013). HuH-7 and Hep3B cell

Downloaded from jpet.aspetjournals.org at ASPET Journals on April 19, 2024

JPET Fast Forward. Published on July 29, 2016 as DOI: 10.1124/jpet.116.235044
This article has not been copyedited and formatted. The final version may differ from this version.

homogenate (50-300 µg of protein) was incubated at 37°C with 500 µM epirubicin hydrochloride for 60 min for UGT2B7, 1 mM of codeine for 90 min for UGT2B4, and 500 µM of nicotine for 14 h for UGT2B10. Epirubicin and nicotine reactions were terminated in the presence of cold 100% acetonitrile while codeine reactions were terminated in the presence of cold 1:1 methanol:acetonitrile. Reactions were centrifuged for 20 min at 13,000 g and supernatant was collected for analysis on UPLC/MS/MS.

Epirubicin-glucuronide formation was analyzed using a Waters ACQUITY ultra-pressure liquid chromatography (UPLC/MS/MS) system (Milford, MA) with a 1.7 µ ACQUITY UPLC BEH C18 analytical column (2.1 mm x 50 mm, Waters, Ireland) in series with a 0.2 µm Waters assay frit filter (2.1 mm). Epirubicin gradient elution conditions were performed using a flow rate of 0.5 mL/min, starting with 95% Buffer A (0.1% formic acid) and 5% Buffer B (0.1% formic acid in acetonitrile) for 30 sec, a subsequent linear gradient to 50% Buffer B over 2.5 min, and then 100% Buffer B maintained over the next 2 min. Epirubicin glucuronides were confirmed by their sensitivity to the treatment of β-glucuronidase. Characterization of epirubicin and epirubicin-glucuronide was conducted using MRM with transitions *m/z* 544 to 130 for epirubicin and *m/z* 720 to 113 for epirubicin-glucuronide. Since an epirubicin-glucuronide standard is not commercially available, quantification was based on the ratio of the area under the curves for epirubicin-glucuronide versus total epirubicin (epirubicin + epirubicin-glucuronide) and the amount of epirubicin (500 µM) added to each glucuronidation assay reaction tube. Data was quantified using the MassLynx™ NT 4.1 software within the QuanLynx™ program (Waters). All experiments were performed three to five times in independent assays.

Codeine gradient elution conditions were performed as described above using a flow rate of 0.5 mL/min, starting with 80% Buffer A (0.1% formic acid) and 20% Buffer B (0.1% formic acid in acetonitrile) for 1 min, followed by 100% Buffer B over the next 2 min, then 20% Buffer B through the remainder of the six min run. The codeine-glucuronide was identified by the

Downloaded from jpet.aspetjournals.org at ASPET Journals on April 19, 2024

JPET Fast Forward. Published on July 29, 2016 as DOI: 10.1124/jpet.116.235044
This article has not been copyedited and formatted. The final version may differ from this version.

transition *m/z* 476.2 to 300.2 and codeine was identified by the single *m/z* of 300.372. Identification of codeine-glucuronide was confirmed by a d_3-labeled codeine-glucuronide internal standard. Quantification was based on a ratio of codeine-glucuronide to codeine in order to maintain consistency across all activity assays for UGT2B enzymes. Data was quantified using the MassLynx™ NT 4.1 software with TargetLynx™ program (Waters). All experiments were performed in triplicate in independent assays.

Nicotine glucuronides were analyzed using a Sciex QTRAP 6500 LC-MS/MS System (Framingham, MA) with a Waters ACQUITY UPLC BEH HILIC 1.7 µm analytic column (2.1 x 100 mm). Nicotine elution gradient conditions were performed with a 0.4 mL/min flow rate, starting with 80% Buffer B (5 mM NH_4Ac in 90% acetonitrile) for 1 min and 50 sec, followed by a steep gradient to 100% Buffer A (5 mM NH_4Ac in 60% acetonitrile) for 3 min, and then back to 80% Buffer B for the remainder of the 10 min run. Identification of nicotine-glucuronide was confirmed by a d_3-labeled codeine-glucuronide internal standard. The transition *m/z* was 339.456 to 163.100 for nicotine-glucuronide and nicotine was identified by the transition m/z of 163.100 to 106 and quantified based on the ratio of nicotine-glucuronide to nicotine using 500 µM per reaction. Data was quantified using the MultiQuant 2.1 Software and performed in triplicate from independent assays.

Statistical Analysis. Statistical analysis was performed using Graphpad Prism 5 software (La Jolla, CA). For all studies involving miR-216b-5p miRNA mimic or miR-216b-5p inhibitors, the Student's t-test (two-tailed) and the linear trend test was used to compare experimental groups with scrambled miRNA controls. For statistical analysis of expression levels of genes labeled B.L.D., a Ct value of 40 was assigned to generate the necessary $2^{-\Delta\Delta C_T}$ values needed for statistical comparison. *P*-values <0.05 were considered statistically significant.

Downloaded from jpet.aspetjournals.org at ASPET Journals on April 19, 2024

JPET Fast Forward. Published on July 29, 2016 as DOI: 10.1124/jpet.116.235044
This article has not been copyedited and formatted. The final version may differ from this version.

Results

miR-216b-5p is predicted to bind to the 3′ UTR of several UGT2B genes. The miRanda and TargetScan miRNA prediction algorithms were used to analyze 3′ UTR sequences from mRNA encoding wild-type, active UGT2B7 (NM_001074), UGT2B4 (NM_021139.2), UGT2B10 (NM_001075.5), UGT2B11 (NM_001073.1), UGT2B15 (NM_001076.2), UGT2B17 (NM_001077.2) and UGT2B28 (NM_053039.1) for potential miRNA binding sites. miR-216b-5p, a conserved miRNA among vertebrates, was the only miRNA candidate to consistently score within the top three predicted miRNA candidates by both programs for several UGT2B genes including UGTs 2B7, 2B4, 2B10, and 2B28. The only prediction score that fell out of the 'top three' for miR-216b-5p was for UGT2B4 predicted by miRanda, where miR-216b-5p was 10th among predicted miRNA candidates. miR-216b-5p was predicted to bind within the 3′ UTR of UGT2B15 by miRanda but not by TargetScan, and was not predicted to bind to the 3′ UTR of UGTs 2B11 or 2B17 by either program. Previous studies have demonstrated high expression of miR-216b-5p in UGT2B-expressing tissues including pancreas, liver, and other metabolic tissues suggesting that this miRNA could be a strong candidate miRNA for regulating UGT2B expression (Endo et al., 2013)

The UGT2B7 3′ UTR contains one potential miR-216b-5p miRNA recognition element (MRE) within its 3′ UTR, located 150 nt from the UGT2B7 stop codon (between nt 1,786 and 1,809 relative to the 5′ end of the UGT2B7 transcript; Fig. 1A). miR-216b-5p MREs were predicted for UGTs 2B4, 2B10, and 2B28 at 65, 136, and 142 nt 3′ of their respective translation stop codons (Fig. 1, panels B-D). All of the predicted miR-216b-5p MREs contained 'seed' sequences of 7 (UGT2B4) or 8 (UGTs 2B7, 2B10, and 2B28) nt of perfect complementarity, which is associated with a greater translation downregulation (Brennecke et al., 2005).

Downloaded from jpet.aspetjournals.org at ASPET Journals on April 19, 2024

JPET Fast Forward. Published on July 29, 2016 as DOI: 10.1124/jpet.116.235044
This article has not been copyedited and formatted. The final version may differ from this version.

Tissue and cell line expression of miR-216b-5p. To determine the levels of expression of miR-216b-5p in tissues and cells with known UGT2B expression, total RNA was screened by real-time PCR. miR-216b-5p expression was highest in pancreas (2,897 ± 166), followed by kidney (4.6 ± 0.98) > liver (3.3 ± 1.62) > breast (1.6 ± 0.46) > trachea (1.1 ± 0.68) > colon (1.0 ± 0.20; set as the reference; Fig. 2). Higher levels of miR-216b-5p were observed in the hepatic HuH-7 cell line (34 ± 8.8) as compared to the Hep3B cell line (1.4 ± 0.27; Fig. 2), with the Hep3B levels comparable to that observed in multiple human tissues including liver. Low levels of miR-216b-5p expression was observed in normal human lung, the lung A-549 cell line and the HEK293 cell line; no expression was detected in normal larynx, jejunum, or endometrium, or in the SK-HEP-1, HepG2, MCF-7 and Caco-2 cell lines (results not shown).

***In vitro* validation of miR-216b-5p target predictions.** *In vitro* validation of the *in silico* miR-216b-5p target predictions was performed for the well-expressed hepatic enzymes, UGTs 2B7, 2B4, and 2B10. Analysis was not performed for UGT2B28 given its low levels of expression in human tissues including human liver (Ohno and Nakajin, 2011). The UGT2B7 3′ UTR was cloned downstream of a luciferase reporter gene and transiently transfected into HEK293 cells with increasing concentrations of miR-216b-5p miRNA mimic. A significant dose-dependent repression of luciferase activity was observed for the UGT2B7 3′ UTR in response to increasing concentrations of miR-216b-5p (P_{trend}<0.0001), with luciferase activity significantly reduced in the presence of 1 nM (P=0.037), 10 nM (P=0.023) and 100 nM (P=0.0071) miR-216b-5p mimic (Fig. 3A, left panel). In order to determine if the predicted UGT2B7 miR-216b-5p MRE is the functional binding site for the interaction between miR-216b-5p and the UGT2B7 3′ UTR, a deletion of 4 nucleotides within the UGT2B7 3′ UTR luciferase vector MRE was made by site-directed mutagenesis (Fig. 1A, underlined). Luciferase activity returned to that of control in the presence of 10 nM miR-216b-5p mimic for HEK293 cells over-expressing the mutated UGT2B7 3′ UTR containing luciferase vector (Fig. 3A, right panel). These results suggest that

Downloaded from jpet.aspetjournals.org at ASPET Journals on April 19, 2024

JPET Fast Forward. Published on July 29, 2016 as DOI: 10.1124/jpet.116.235044
This article has not been copyedited and formatted. The final version may differ from this version.

miR-216b-5p is functionally binding to the predicted MRE on the UGT2B7 3′ UTR and that the interaction causes a decrease in expression of the luciferase gene.

Similar to that observed for UGT2B7, a significant dose-dependent repression of luciferase activity in response to increasing concentrations of miR-216b-5p after transfection of HEK293 cells was observed for both the UGT2B4 (P_{trend}<0.0001) and UGT2B10 (P_{trend}<0.0001) 3′ UTRs. For the UGT2B4 3′ UTR, the reduction of luciferase activity was significant at 10 nM (P=0.024) and 100 nM (P=0.031) of miR-216b-5p, (Fig. 3, panel B left panel). The luciferase activity of cell homogenates transfected with the UGT2B10 3′ UTR-containing vector decreased at 1 nM (P=0.020), 10 nM (P=0.010), and 100 nM (P=0.0018) of miR-216b-5p (Fig. 3, panel C, left panel). Deletion of 4 nucleotides within the predicted miR-216b-5p 'seed' sequences of each of the UGT2B 3′ UTR-containing luciferase vectors resulted in a reversal of this repression (Fig. 3B and Fig. 3C, right panels). These results validate the *in silic*o data and suggest that miR-216b-5p can bind with multiple UGT2B mRNAs.

A functional miR-216b-5p binding site polymorphism in the UGT2B10 3′ UTR.

Analysis of the UGT2B10 3′ UTR mRNA sequence within the SNP 500 Cancer Project database (Packer et al., 2004) identified a low prevalence (~1% in Caucasians) single nucleotide polymorphism (SNP; rs139538767) consisting of an adenine (A) to guanine (G) transition located within the predicted miR-216b-5p MRE of the 3′ UTR of UGT2B10 (Fig. 1C; bold, underlined). A UGT2B10 3′ UTR luciferase reporter vector containing the G variant was created to ascertain whether this polymorphism conferred an effect on the binding of miR-216b-5p. In contrast to the significant repression of luciferase activity observed with the wild-type UGT2B10 3′ UTR, the G variant UGT2B10 3′ UTR exhibited no repression of luciferase activity, a pattern similar to that observed for the 'seed' deletion control (Fig. 3C, right panel). These data suggest that SNPs in MREs lying within a UGT mRNA 3′ UTR could potentially result in differential regulation of UGT expression and possibly glucuronidation activities between individuals.

Downloaded from jpet.aspetjournals.org at ASPET Journals on April 19, 2024

JPET Fast Forward. Published on July 29, 2016 as DOI: 10.1124/jpet.116.235044
This article has not been copyedited and formatted. The final version may differ from this version.

Effects of miR-216b-5p on UGT2B mRNA expression in hepatic cell lines. The relative expression levels of UGT2B7, UGT2B4, and UGT2B10 were examined in the HuH-7 and Hep3B cell lines. HuH-7 and Hep3B cells were chosen because both cell lines express multiple UGT2B enzymes (Guo et al., 2011) and endogenously express miR-216b-5p (Fig. 2), and could therefore potentially serve as an *in vitro* model for miR-216b-5p UGT2B interactions. As determined by qRT-PCR, UGT2B4 exhibited the highest level of mRNA expression of any UGT2B isoform, with Hep3B UGT2B4 mRNA expression the highest overall in both cell lines (reference set at 1.0; Fig. 4). In HuH-7 cells, UGT2B4 expression levels were 63% that of Hep3B UGT2B4 mRNA levels; UGT2B7 expression was 0.07 (Hep3B) and 0.12 (HuH-7) that observed for UGT2B4 in Hep3B cells, while UGT2B10 expression was very low in both cell lines.

In order to determine if miR-216b-5p interacts with endogenous UGT2B mRNAs, 50 nM of miR-216b-5p miRNA mimic was transfected into the HuH-7 and Hep3B cell lines and mRNA levels were determined by qRT-PCR. Decreases in the mRNA levels were observed after over-expression of miR-216b-5p in HuH-7 and Hep3B cells for UGTs 2B7, 2B4 and 2B10 (Fig. 5). Significant decreases were observed for UGT2B7 in HuH-7 cells (P<0.001; Fig. 5A), UGT2B4 in Hep3B cells (P<0.001; Fig 5B) and UGT2B10 in both cell lines (P=0.0018 for HuH-7 cells and P=0.018 for HepG2 cells; Fig. 5, panels A and B, respectively). No effect was observed for other hepatic UGT2B enzymes including UGTs 2B11, 2B15, and 2B17 in either cell line after over-expression of miR-216b-5p (results not shown).

To examine the endogenous effects of miR-216b-5p on UGT2B mRNA levels, 100 nM of miRNA miR-216b-5p inhibitor was used to transiently inhibit miR-216b-5p function in both cell lines. Endogenous levels of miR-216b-5p were significantly repressed by 100- (P=0.026) and 25- (P=0.0045) fold in HuH-7 and Hep3B cells, respectively, (Fig. 5, panels C and D). The mRNA levels of each UGT2B isoform was quantified using qRT-PCR analysis to measure the

Downloaded from jpet.aspetjournals.org at ASPET Journals on April 19, 2024

JPET Fast Forward. Published on July 29, 2016 as DOI: 10.1124/jpet.116.235044
This article has not been copyedited and formatted. The final version may differ from this version.

effect on mRNA expression when endogenous miR-216b-5p is inhibited. UGT2B7 mRNA levels were significantly increased in both HuH-7 (P=0.021) and Hep3B (P=0.0068) cells in the presence of the miR-216b-5p inhibitor (Fig. 5, panels E and F). A significant (P<0.001) increase in mRNA levels was also observed for UGT2B4 when miR-216b-5p was inhibited in HuH-7 cells (Fig. 5E). Interestingly, UGT2B10 mRNA levels were significantly repressed in both cell lines when miR-216b-5p was inhibited (Fig. 5, panels E and F).

Effect of miR-216b-5p on UGT2B protein levels and activity in hepatic cell lines. To investigate the effect of miR-216b-5p over-expression on UGT2B enzymatic activity, HuH-7 and Hep3B cells were transiently transfected with miR-216b-5p mimic and UGT2B protein expression and/or enzymatic activities were assessed. While useful specific antibodies are not available for most UGT2B enzymes (including UGT2B4 and UGT2B10), a sensitive and specific antibody is available from BD Biosciences (San Jose, CA) for the detection of UGT2B7. Using this antibody in Western blot analysis, a 47% decrease in UGT2B7 protein after transfection with 100 nM miR216b was observed (Fig. 6A). This corresponded with significant decreases in UGT2B7 glucuronidation activity (Fig. 6B). Using the UGT2B7-specific substrate epirubicin (Innocenti et al., 2001; Zaya et al., 2006), a significant (P_{trend}<0.001) dose-dependent decrease in epirubicin glucuronidation was observed in assays with 500 µM epirubicin. As compared to the scrambled miRNA control, there was a significant (P=0.023) 29% reduction in glucuronide formation in HuH-7 cells transfected with 10 nM of miR-216b-5p, a significant (P=0.018) 49% reduction at 50 nM of miR-216b-5p, and a significant (P<0.0001) 58% reduction at 100 nM of miR-216b-5p. A similar pattern was observed in Hep3B cells, with a 21% decrease in UGT2B7 protein expression (Fig. 6C) and a significant (P=0.011) 35% decrease in epirubicin glucuronidation after transient transfection with 50 nM miR-216b-5p (Fig. 6D).

To examine the impact of endogenous miR-216b-5p expression on the regulation of UGT2B7 in HuH-7 and Hep3B cells, transient transfection with 100 nM miR-216b-5p inhibitor

Downloaded from jpet.aspetjournals.org at ASPET Journals on April 19, 2024

JPET Fast Forward. Published on July 29, 2016 as DOI: 10.1124/jpet.116.235044
This article has not been copyedited and formatted. The final version may differ from this version.

was performed to significantly inhibit miR-216b-5p endogenous expression in the two cell lines. An increase of >60% in the levels of UGTB7 protein was observed in miR-216b-5p-inhibited HuH-7 cells (Fig. 6E) and this corresponded with a near-significant increase (~85%; *P*=0.0572) in epirubicin glucuronidation activity (Fig. 6F). Similar results were seen in Hep3B cells, where UGT2B7 protein expression increased by 45% (Fig. 6G) and epirubicin glucuronidation levels were significantly (*P*=0.012) increased by 50% (Fig. 6H).

The effect of miR-216b-5p on UGT2B4 enzyme activity was measured via glucuronidation activity against codeine. While UGTs 2B4 and 2B7 are the two UGTs that exhibit significant and roughly equivalent levels of activity against codeine (Court et al., 2003), UGT2B4 is expressed at approximately 5- and 14-times greater levels than UGT2B7 in HuH-7 and Hep3B cells, respectively (see Fig. 4), suggesting that codeine-glucuronide formation is likely driven primarily by UGT2B4 in both cell lines. Possibly due to high expression of UGT2B4 in HuH-7 cells (see Fig. 4), higher concentrations (50-250 nM) of miR-216b-5p were required for transfection to observe an effect on UGT2B4 expression. In HuH-7 cells, codeine-glucuronide formation was significantly decreased by 52% (*P*<0.001) and 54% (*P*<0.001) at 125 nM and 250 nM, respectively, with a linear trend towards decreased codeine-glucuronide formation observed with increasing concentrations of miR-216b-5p (P_{trend}<0.001; Fig. 6I). In Hep3B cells, the decrease in codeine-glucuronide formation was 28% (*P*=0.040), 34% (*P*=0.027) and 46% (*P*=0.0090) for 10 nM, 25 nM and 50 nM, respectively, with a significant trend towards decreased codeine glucuronidation with increased miR-216b-5p (P_{trend}=0.0048; Fig. 6J).

Nicotine was shown to be a selective substrate for UGT2B10 in previous studies (Chen et al., 2007; Chen et al., 2008). Activity assays utilizing nicotine were used to evaluate the effect of increasing concentrations of miR-216b-5p on UGT2B10 activity. A significant trend (P_{trend}=0.0035) towards decreasing nicotine-glucuronide formation was observed in HuH-7 cells with increasing concentrations of miR-216b-5p, with a reduction in nicotine-glucuronide

Downloaded from jpet.aspetjournals.org at ASPET Journals on April 19, 2024

JPET Fast Forward. Published on July 29, 2016 as DOI: 10.1124/jpet.116.235044
This article has not been copyedited and formatted. The final version may differ from this version.

formation of 31% (*P*=0.017) at 100 nM miR-216b-5p (Fig. 6K). Similarly, Hep3B nicotine glucuronidation activity was significantly (*P*=0.043) decreased by 47% at 50 nM of miR-216b-5p (Fig. 6L). These results indicated that miR-216b-5p's interaction with UGT2B 3′ UTRs affects enzymatic activity.

Downloaded from jpet.aspetjournals.org at ASPET Journals on April 19, 2024

JPET Fast Forward. Published on July 29, 2016 as DOI: 10.1124/jpet.116.235044
This article has not been copyedited and formatted. The final version may differ from this version.

Discussion

This is the first study identifying a miRNA regulator of UGTs 2B7, 2B4 and 2B10. *In silico* miRNA prediction programs were used to identify miR-216b-5p binding motifs within the 3′ UTRs of several UGT2B enzymes including UGT2B4, UGT2B7, UGT2B10, and UGT2B28. Results from this *in silico* analysis were validated by *in vitro* over-expression studies of luciferase vectors containing wild-type or mutated UGT2B 3′ UTR MRE sequences, suggesting that *in silico* prediction modeling is a useful tool to predict miRNA-gene interactions within the UGT gene family. While UGT2B28 was not examined experimentally in the present study, over-expression of 10 nM miR-216b-5p resulted in a significant decrease in luciferase activity using vectors containing the UGT2B28 3′ UTR in previous studies (Margaillan et al., 2016).

The positioning of the miR-216b-5p MREs for each UGT2B mRNA are all located between 65 and 150 nt downstream of their respective translation stop codons, and this is likely related to sequence similarities within the UGT2B gene locus. It has been hypothesized that gene duplication events created the UGT2B gene family, with UGT2B4 being an ancestral gene (Guillemette et al., 2010). Therefore, it is likely that miR-216b-5p binding sites were duplicated and conserved during this process.

The seed sequence for miR-216b-5p shares seven of eight nucleotides with the seed sequence for the closely related miR-216a-5p. There is no predicated binding site for miR-216a-5p for UGT2B4. Both UGT2B7 and UGT2B10 have a predicted binding site for miR-216a-5p that overlap the stop codon, with UGT2B10 having a second predicted miR-216a-5p binding site 504 nt 3′ of the UGT2B10 stop codon. While it is possible that miR-216b-5p is binding to miR-216a-5p sites, the luciferase data presented in this study indicate that binding to an alternative site is likely minimal. In unpublished studies (Dluzen and Lazarus), miR-216a-5p mimic reduced

Downloaded from jpet.aspetjournals.org at ASPET Journals on April 19, 2024

JPET Fast Forward. Published on July 29, 2016 as DOI: 10.1124/jpet.116.235044
This article has not been copyedited and formatted. The final version may differ from this version.

luciferase activity for both UGT2B7 and UGT2B10 but not UGT2B4, and no significant effect on UGT2B expression or protein activity was observed in HuH-7 or Hep3B cells, suggesting that miR-216a-5p is not a major regulator of UGT2B expression/activity.

miR-216b-5p expression levels were quantified in several UGT-expressing tissues, with miR-216b-5p exhibiting moderate expression in liver, and highest expression in pancreas. These results are consistent with data from the only other previous study investigating tissue expression of miR-216b-5p where high hepatic and pancreatic expression of miR-216b-5p was also observed (Endo et al., 2013). The fact that miR-216b-5p is expressed hepatically is consistent with a potential role in the regulation of hepatic UGT2B expression and in drug metabolism.

Although miR-216b has not been previously linked with drug metabolism, miR-216b serves as a tumor-suppressor in liver cancer cells by regulating expression of insulin-like 2 mRNA-binding protein 2 (IGF2BP) and influencing downstream AKT/mTOR and MAPK signaling pathways(Liu et al., 2015). miR-216b levels were shown to be lower in patients with hepatocellular carcinoma (HCC) and higher expression is associated with increased 5-year survival (Liu et al., 2015). miR-216b targets FGFR1 in pancreatic cancer cells and decreased expression is a marker for poor prognosis in pancreatic patients (Egeli et al., 2016).

In vitro over-expression of miR-216b-5p in the HuH-7 and Hep3B hepatocellular carcinoma cell lines resulted in decreased mRNA expression of the three hepatically-expressed UGT2B enzymes (UGTs 2B7, 2B4, and 2B10) predicted by *in silico* models to bind miR-216b-5p. Interestingly, similar decreases in mRNA expression were not observed for several other hepatic UGT2B enzymes after over-expression of miR-216b-5p including UGTs 2B11, 2B15, and 2B17. This is consistent with the fact that none of these latter UGTs were predicted to bind miR-216b-5p *in silico*. For UGTs 2B7 and 2B4, these results were corroborated by *in vitro*

Downloaded from jpet.aspetjournals.org at ASPET Journals on April 19, 2024

JPET Fast Forward. Published on July 29, 2016 as DOI: 10.1124/jpet.116.235044
This article has not been copyedited and formatted. The final version may differ from this version.

studies where endogenous miR-216b-5p was depleted using a miR-216b-5p inhibitor, resulting in the up-regulation of mRNA levels for both UGTs 2B7 and 2B4 in at least one or both of the hepatocellular carcinoma cell lines tested. The decrease in UGT2B10 expression observed in the presence of the miR-216b-5p inhibitor may be due to the presence of another miRNA that binds to and competes for the same miR-216b-5p miRNA-binding site. *In silico* analysis of UGT2B10 by both miRanda and TargetScan reveals that miR-379 is predicted to bind to UGT2B10 within eight nucleotides of the miR216b MRE but is not predicted to bind the 3′ UTRs of both UGTs 2B4 and 2B7. Further studies are required to address this possibility.

The inhibitory pattern observed for miR-216b-5p on UGT2B mRNA expression was also observed for UGT2B7 protein. Epirubicin glucuronidation is primarily mediated by UGT2B7 (Innocenti et al., 2001; Zaya et al., 2006) and miR-216b-5p over-expression significantly reduced epirubicin glucuronide formation in both HuH-7 and Hep3B cells. In addition, depletion of endogenous miR-216b-5p using a miR-216b-5p-specific inhibitor increased UGT2B7 protein levels and activity in both cell lines. The same pattern of reduced glucuronidation activity after over-expression of miR-216 mimic was observed against codeine, a substrate of UGT2B4 (Court et al., 2003), as well as nicotine, a substrate of UGT2B10 (Chen et al., 2007; Chen et al., 2008). Together with the fact that miR-216b-5p over-expression also decreased UGTs 2B7, 2B4 and 2B10 mRNA expression levels, these data indicate that endogenous miR-216b-5p may play a role in UGT2B functionality and suggests a potential regulatory mechanism in normal human liver and perhaps other tissues where UGTs 2B7, 2B4 and 2B10 are co-expressed with miR-216b-5p.

Interestingly, a larger increase in UGT2B7 protein activity was observed in HuH-7 cells compared with Hep3B cells when endogenous miR-216b-5p was inhibited. This may reflect the fact that endogenous miR-216b-5p expression levels are >30-fold higher in HuH-7 cells compared to Hep3B cells and relief from miR-216b-5p regulation would thus impact UGT2B7

Downloaded from jpet.aspetjournals.org at ASPET Journals on April 19, 2024

JPET Fast Forward. Published on July 29, 2016 as DOI: 10.1124/jpet.116.235044
This article has not been copyedited and formatted. The final version may differ from this version.

expression to a greater extent in HuH-7 cells. The normal human liver tissue samples used in this study had only approximately 2-fold higher endogenous miR-216b-5p expression compared to Hep3B cells. An approximately 25% increase in UGT2B7 glucuronidation in Hep3B cells with inhibited miR-216b-5p, and this may better reflect the endogenous repression of UGT2B7 in normal liver.

Interestingly, there is a known SNP within the miR-216b-5p MRE 'seed' sequence of the UGT2B10 3′ UTR (rs139538767). This polymorphism functions in a manner similar to that observed for the UGT2B10 3′ UTR seed deletion control, resulting in an elimination of the negative regulation of UGT2B10 3′ UTR luciferase expression after miR-216b-5p over-expression. These data suggest that this SNP may cause altered regulation of the polymorphic UGT2B10 allele. The minor allele frequency of this SNP is low, with a prevalence of ~1% in the Caucasian population, but the present study provides the first evidence of a UGT2B 3′ UTR SNP with a direct functional role in aberrant miRNA regulation.

In summary, we provide evidence of a functional miR-216b-5p binding motif within the 3′ UTR of several UGT2B isoforms. UGT2B7 and UGT2B4 mRNA and protein expression, as well as overall enzymatic activity, were significantly repressed in the presence of over-expressed miR-216b-5p and were induced after the addition of miR-216b-5p inhibitor, and this may have functional consequences on UGT2B7 and UGT2B4 enzymatic activity *in vivo*. UGT2B10 mRNA levels and glucuronidation activity were also reduced in the presence of the miR-216b-5p mimic. In addition, a functional SNP was identified in the UGT2B10 3′ UTR which may modify UGT2B10 regulation through a miR-216b-5p-mediated pathway. Together, these data suggest that miR-216b-5p may exhibit a regulatory function on the overall glucuronidation activity of several UGT2B enzymes and that changes in miR-216b-5p expression or the presence of SNPs in miR-216b-5p-binding motifs in UGT2B 3′ UTRs may contribute to inter-individual variability of UGT2B expression and affect overall phase II metabolism in humans.

Downloaded from jpet.aspetjournals.org at ASPET Journals on April 19, 2024

JPET Fast Forward. Published on July 29, 2016 as DOI: 10.1124/jpet.116.235044
This article has not been copyedited and formatted. The final version may differ from this version.

Acknowledgements

We would like to thank the Washington State University Mass Spectrometry Core Facility for their support and help with analysis of glucuronide detection. We acknowledge the assistance and help of the Amity Platt for her advice and help in refining molecular techniques.

Downloaded from jpet.aspetjournals.org at ASPET Journals on April 19, 2024

JPET Fast Forward. Published on July 29, 2016 as DOI: 10.1124/jpet.116.235044
This article has not been copyedited and formatted. The final version may differ from this version.

References

Baek D, Villen J, Shin C, Camargo FD, Gygi SP and Bartel DP (2008) The impact of microRNAs on protein output. *Nature* **455**:64-71.

Bartel DP (2009) MicroRNAs: target recognition and regulatory functions. *Cell* **136**:215-233.

Betel D, Wilson M, Gabow A, Marks DS and Sander C (2008) The microRNA.org resource: targets and expression. *Nucleic Acids Res* **36**:D149-153.

Brennecke J, Stark A, Russell RB and Cohen SM (2005) Principles of microRNA-target recognition. *PLoS Biol* **3**:e85.

Brodersen P and Voinnet O (2009) Revisiting the principles of microRNA target recognition and mode of action. *Nat Rev Mol Cell Biol* **10**:141-148.

Carthew RW and Sontheimer EJ (2009) Origins and Mechanisms of miRNAs and siRNAs. *Cell* **136**:642-655.

Chen G, Blevins-Primeau AS, Dellinger RW, Muscat JE and Lazarus P (2007) Glucuronidation of nicotine and cotinine by UGT2B10: loss of function by the UGT2B10 Codon 67 (Asp>Tyr) polymorphism. *Cancer Res* **67**:9024-9029.

Chen G, Dellinger RW, Sun D, Spratt TE and Lazarus P (2008) Glucuronidation of tobacco-specific nitrosamines by UGT2B10. *Drug Metab Dispos* **36**:824-830.

Chouinard S, Barbier O and Belanger A (2007) UDP-glucuronosyltransferase 2B15 (UGT2B15) and UGT2B17 enzymes are major determinants of the androgen response in prostate cancer LNCaP cells. *J Biol Chem* **282**:33466-33474.

Court MH, Krishnaswamy S, Hao Q, Duan SX, Patten CJ, Von Moltke LL and Greenblatt DJ (2003) Evaluation of 3'-azido-3'-deoxythymidine, morphine, and codeine as probe substrates for UDP-glucuronosyltransferase 2B7 (UGT2B7) in human liver microsomes: specificity and influence of the UGT2B7*2 polymorphism. *Drug metabolism and disposition: the biological fate of chemicals* **31**:1125-1133.

Dellinger RW, Chen G, Blevins-Primeau AS, Krzeminski J, Amin S and Lazarus P (2007) Glucuronidation of PhIP and N-OH-PhIP by UDP-glucuronosyltransferase 1A10. *Carcinogenesis* **28**:2412-2418.

Dluzen DF, Sun D, Salzberg AC, Jones N, Bushey RT, Robertson GP and Lazarus P (2014) Regulation of UGT1A1 expression and activity by miR-491-3p. *J Pharmacol Exp Ther*.

Egeli U, Tezcan G, Cecener G, Tunca B, Demirdogen Sevinc E, Kaya E, Ak S, Dundar HZ, Sarkut P, Ugras N, Yerci O, Ozen Y and Evrensel T (2016) miR-216b Targets FGFR1 and Confers Sensitivity to Radiotherapy in Pancreatic Ductal Adenocarcinoma Patients Without EGFR or KRAS Mutation. *Pancreas*.

Endo K, Weng H, Kito N, Fukushima Y and Iwai N (2013) MiR-216a and miR-216b as markers for acute phased pancreatic injury. *Biomed Res* **34**:179-188.

Garcia DM, Baek D, Shin C, Bell GW, Grimson A and Bartel DP (2011) Weak seed-pairing stability and high target-site abundance decrease the proficiency of lsy-6 and other microRNAs. *Nat Struct Mol Biol* **18**:1139-1146.

Guillemette C, Levesque E, Harvey M, Bellemare J and Menard V (2010) UGT genomic diversity: beyond gene duplication. *Drug Metab Rev* **42**:24-44.

Guo H, Ingolia NT, Weissman JS and Bartel DP (2010) Mammalian microRNAs predominantly act to decrease target mRNA levels. *Nature* **466**:835-840.

Guo L, Dial S, Shi L, Branham W, Liu J, Fang JL, Green B, Deng H, Kaput J and Ning B (2011) Similarities and differences in the expression of drug-metabolizing enzymes between human hepatic cell lines and primary human hepatocytes. *Drug Metab Dispos* **39**:528-538.

Downloaded from jpet.aspetjournals.org at ASPET Journals on April 19, 2024

JPET Fast Forward. Published on July 29, 2016 as DOI: 10.1124/jpet.116.235044
This article has not been copyedited and formatted. The final version may differ from this version.

Innocenti F, Iyer L, Ramirez J, Green MD and Ratain MJ (2001) Epirubicin glucuronidation is catalyzed by human UDP-glucuronosyltransferase 2B7. *Drug Metab Dispos* **29**:686-692.

Itaaho K, Mackenzie PI, Ikushiro S, Miners JO and Finel M (2008) The configuration of the 17-hydroxy group variably influences the glucuronidation of beta-estradiol and epiestradiol by human UDP-glucuronosyltransferases. *Drug Metab Dispos* **36**:2307-2315.

Izukawa T, Nakajima M, Fujiwara R, Yamanaka H, Fukami T, Takamiya M, Aoki Y, Ikushiro S, Sakaki T and Yokoi T (2009) Quantitative analysis of UDP-glucuronosyltransferase (UGT) 1A and UGT2B expression levels in human livers. *Drug Metab Dispos* **37**:1759-1768.

Jones NR and Lazarus P (2014) UGT2B gene expression analysis in multiple tobacco carcinogen-targeted tissues. *Drug Metab Dispos* **42**:529-536.

Lewis BP, Burge CB and Bartel DP (2005) Conserved seed pairing, often flanked by adenosines, indicates that thousands of human genes are microRNA targets. *Cell* **120**:15-20.

Liu FY, Zhou SJ, Deng YL, Zhang ZY, Zhang EL, Wu ZB, Huang ZY and Chen XP (2015) MiR-216b is involved in pathogenesis and progression of hepatocellular carcinoma through HBx-miR-216b-IGF2BP2 signaling pathway. *Cell Death Dis* **6**:e1670.

Livak KJ and Schmittgen TD (2001) Analysis of relative gene expression data using real-time quantitative PCR and the 2(-Delta Delta C(T)) Method. *Methods* **25**:402-408.

Mackenzie PI, Bock KW, Burchell B, Guillemette C, Ikushiro S, Iyanagi T, Miners JO, Owens IS and Nebert DW (2005) Nomenclature update for the mammalian UDP glycosyltransferase (UGT) gene superfamily. *Pharmacogenet Genomics* **15**:677-685.

Mackenzie PI, Hu DG and Gardner-Stephen DA (2010) The regulation of UDP-glucuronosyltransferase genes by tissue-specific and ligand-activated transcription factors. *Drug Metab Rev* **42**:99-109.

Margaillan G, Levesque E and Guillemette C (2016) Epigenetic regulation of steroid inactivating UDP-glucuronosyltransferases by microRNAs in prostate cancer. *J Steroid Biochem Mol Biol* **155**:85-93.

Mukherji S, Ebert MS, Zheng GX, Tsang JS, Sharp PA and van Oudenaarden A (2011) MicroRNAs can generate thresholds in target gene expression. *Nat Genet* **43**:854-859.

Nakamura A, Nakajima M, Yamanaka H, Fujiwara R and Yokoi T (2008) Expression of UGT1A and UGT2B mRNA in human normal tissues and various cell lines. *Drug Metab Dispos* **36**:1461-1464.

Ohno S and Nakajin S (2009) Determination of mRNA expression of human UDP-glucuronosyltransferases and application for localization in various human tissues by real-time reverse transcriptase-polymerase chain reaction. *Drug Metab Dispos* **37**:32-40.

Ohno S and Nakajin S (2011) Quantitative analysis of UGT2B28 mRNA expression by real-time RT-PCR and application to human tissue distribution study. *Drug metabolism letters* **5**:202-208.

Ohtsuki S, Schaefer O, Kawakami H, Inoue T, Liehner S, Saito A, Ishiguro N, Kishimoto W, Ludwig-Schwellinger E, Ebner T and Terasaki T (2012) Simultaneous absolute protein quantification of transporters, cytochromes P450, and UDP-glucuronosyltransferases as a novel approach for the characterization of individual human liver: comparison with mRNA levels and activities. *Drug Metab Dispos* **40**:83-92.

Packer BR, Yeager M, Staats B, Welch R, Crenshaw A, Kiley M, Eckert A, Beerman M, Miller E, Bergen A, Rothman N, Strausberg R and Chanock SJ (2004) SNP500Cancer: a public resource for sequence validation and assay development for genetic variation in candidate genes. *Nucleic Acids Res* **32**:D528-532.

Pan YZ, Gao W and Yu AM (2009) MicroRNAs regulate CYP3A4 expression via direct and indirect targeting. *Drug Metab Dispos* **37**:2112-2117.

Downloaded from jpet.aspetjournals.org at ASPET Journals on April 19, 2024

JPET Fast Forward. Published on July 29, 2016 as DOI: 10.1124/jpet.116.235044
This article has not been copyedited and formatted. The final version may differ from this version.

Riedy M, Wang JY, Miller AP, Buckler A, Hall J and Guida M (2000) Genomic organization of the UGT2b gene cluster on human chromosome 4q13. *Pharmacogenetics* **10**:251-260.

Sato Y, Nagata M, Kawamura A, Miyashita A and Usui T (2012) Protein quantification of UDP-glucuronosyltransferases 1A1 and 2B7 in human liver microsomes by LC-MS/MS and correlation with glucuronidation activities. *Xenobiotica* **42**:823-829.

Stingl JC, Bartels H, Viviani R, Lehmann ML and Brockmoller J Relevance of UDP-glucuronosyltransferase polymorphisms for drug dosing: A quantitative systematic review. *Pharmacol Ther*.

Sun D, Jones NR, Manni A and Lazarus P (2013) Characterization of raloxifene glucuronidation. Potential role of UGT1A8 genotype on raloxifene metabolism in vivo. *Cancer Prev Res (Phila)*.

Sun D, Sharma AK, Dellinger RW, Blevins-Primeau AS, Balliet RM, Chen G, Boyiri T, Amin S and Lazarus P (2007) Glucuronidation of active tamoxifen metabolites by the human UDP glucuronosyltransferases. *Drug Metab Dispos* **35**:2006-2014.

Wijayakumara DD, Hu DG, Meech R, McKinnon RA and Mackenzie PI (2015) Regulation of Human UGT2B15 and UGT2B17 by miR-376c in Prostate Cancer Cell Lines. *J Pharmacol Exp Ther* **354**:417-425.

Zaya MJ, Hines RN and Stevens JC (2006) Epirubicin glucuronidation and UGT2B7 developmental expression. *Drug Metab Dispos* **34**:2097-2101.

Downloaded from jpet.aspetjournals.org at ASPET Journals on April 19, 2024

JPET Fast Forward. Published on July 29, 2016 as DOI: 10.1124/jpet.116.235044
This article has not been copyedited and formatted. The final version may differ from this version.

Footnotes

1. D.F. Dluzen and A.K. Sutliff contributed equally to this work as co-first authors.

2. Funding: This work was funded in part by a student fellowship provided by AstraZeneca (to D Dluzen), and grants from the National Institutes of Health, National Institute of Dental and Craniofacial Research [grant R01-DE13158 to P Lazarus] and the National Institutes of Environmental Health Sciences [grant R01-ES025460 to P Lazarus].

3. Authorship Contributions:

   Participated in research design: Dluzen, Sutliff, Chen, Watson, Ishmael, and Lazarus

   Conducted experiments: Dluzen and Sutliff

   Contributed new reagents or analytic tools: Dluzen, Sutliff, Chen, Watson, Ishmael, and Lazarus

   Performed data analysis: Dluzen, Sutliff, Chen, Watson, Ishmael, and Lazarus

   Wrote or contributed to writing of the manuscript: Dluzen, Sutliff, Chen, Watson, Ishmael, and Lazarus

4. Reprint requests: Philip Lazarus, Ph.D., Department of Pharmaceutical Sciences, Washington State University College of Pharmacy, PO Box 1495, Spokane, WA, 99202; Email: phil.lazarus@wsu.edu

Downloaded from jpet.aspetjournals.org at ASPET Journals on April 19, 2024

JPET Fast Forward. Published on July 29, 2016 as DOI: 10.1124/jpet.116.235044
This article has not been copyedited and formatted. The final version may differ from this version.

Figure Legends

Figure 1. ***In silico*** **prediction and binding of miR-216b-5p to UGT2B isoforms.** The miRNA prediction algorithms miRanda and TargetScan were used to identify miRNA binding candidates for all seven UGT2B isoform mRNAs. miR-216b-5p is predicted to bind to a 3′ UTR MRE located within each of the UGT2B7 (panel *A*), UGT2B4 (panel *B*), UGT2B10 (panel *C*), and UGT2B28 (panel *D*) 3′ UTR mRNA sequences (black bars). The canonical 'seed' sequences of the predicted hybridization between miR-216b-5p and each 3′ UTR are located underneath each gene and underlined in black. The nucleotide that constitutes a SNP within the UGT2B10 MRE is in bold.

Figure 2. Tissue and cell line expression of miR-216b-5p. Expression levels of miR-216b-5p were quantified using qRT-PCR and set relative to the lowest-expressing tissue (i.e. colon). miR-216b-5p expression is adjusted to the RNU6B endogenous control gene in the same samples. The Y-axis is broken into two segments, with a gap between 45 and 2000 to better adjust for the high expression levels quantified in the pancreas. The mean Ct values are listed below the table. Columns represent the mean ± S.E. of three independent replicates.

Figure 3. UGT2B 3′ UTR luciferase activity in the presence of miR-216b-5p mimics. Luciferase activity of the UGT2B7 (panel *A*, left), UGT2B4 (panel *B*, left), and UGT2B10 (panel *C*, left) 3′ UTR luciferase reporter vectors co-transfected with increasing concentrations of miR-216b-5p mimic or scrambled (100 nM) miRNA control in HEK293

Downloaded from jpet.aspetjournals.org at ASPET Journals on April 19, 2024

JPET Fast Forward. Published on July 29, 2016 as DOI: 10.1124/jpet.116.235044
This article has not been copyedited and formatted. The final version may differ from this version.

cells. Luciferase activity was also examined in the presence of 10 nM scrambled or miR-216b-5p mimic after each UGT2B miRNA response element was mutated within the miR-216b-5p 'seed' sequence ('seed' deletion columns; right panels). Luciferase activity of the UGT2B10 3′ UTR variant SNP in the presence of 10 nM miR-216b-5p was also measured (panel *C*, right). Columns represent mean ± S.E. of at least three independent experiments and are normalized to the scrambled miRNA-transfected control. * $P<0.05$; ** $P<0.01$; *** $P<0.001$.

Figure 4. UGT2B mRNA expression in HuH-7 and Hep3B cells. UGT2B mRNA expression was quantified in HuH-7 and Hep3B cells using qRT-PCR. mRNA expression was determined using RPLP0 as an internal endogenous control and expressed relative to the highest expressing UGT2B mRNA transcript, UGT2B4, in Hep3B cells (set at 1.0 as the reference). The Y-axis contains a gap between 0.15 and 0.50 to better adjust for high UGT2B4 expression levels. Columns represent mean ± S.E. of three independent replicates.

Figure 5. UGT2B mRNA levels in HuH-7 and Hep3B cells with miR-216b-5p mimic or inhibitor. mRNA levels of UGT2B7, UGT2B4, and UGT2B10 in HuH-7 (panel *A*) and Hep3B (panel *B*) cells after transfection with 50 nM scrambled or miR-216b-5p mimic were quantified by qRT-PCR relative to the endogenous internal control gene RPLP0. mRNA levels for each gene are shown relative to the scrambled control (set at 1.0 as the reference). Endogenous expression levels of miR-216b-5p were quantified using qRT-PCR in the presence of 100 nM scrambled or miR-216b-5p inhibitor in HuH-7 (panel *C*) and Hep3B (panel *D*) cells. miR-216b-5p expression levels were quantified against the

Downloaded from jpet.aspetjournals.org at ASPET Journals on April 19, 2024

JPET Fast Forward. Published on July 29, 2016 as DOI: 10.1124/jpet.116.235044
This article has not been copyedited and formatted. The final version may differ from this version.

RNU6B endogenous internal miRNA control gene and each gene is shown relative to the scrambled miRNA inhibitor control (set as 1.0). The mRNA expression levels of UGT2B7, UGT2B4, and UGT2B10 were quantified using qRT-PCR in the presence of 100 nM scrambled or miR-216b-5p inhibitor in HuH-7 (panel *E*) and Hep3B (panel *F*) cells. Each gene was quantified against the endogenous internal control gene RPLP0 and each gene is shown relative to the scrambled miRNA inhibitor control (set as 1.0). Columns represent mean ± S.E. of three independent experiments. * $P<0.05$; ** $P<0.01$; *** $P<0.001$.

Figure 6. UGT2B7 protein expression and UGT2B glucuronidation activity in the presence of miR-216b-5p mimic or inhibitor. Panel *A*; Representative blot of HuH-7 UGT2B7 protein expression after transfection of 10 nM, 50 nM, or 100 nM miR-216b-5p mimic or 100 nM of scrambled miRNA mimic control. UGT2B7 protein bands were normalized to β-actin band intensities and compared to normalized UGT2B7 protein bands from cells transfected with scrambled miRNA control. Panel *B*; UGT2B7 glucuronidation activity against epirubicin in HuH-7 cells transfected with 10 nM, 50 nM, or 100 nM miR-216b-5p mimic or 100 nM of scrambled miRNA control. Panel *C*, Top; Representative blot of Hep3B UGT2B7 protein expression in the presence of 50 nM of scrambled control or miR-216b-5p mimic. Panel D; UGT2B7 glucuronidation activity against epirubicin in Hep3B cells transfected with 50 nM scrambled or miR-216b-5p mimic. Panel *E*; Representative blot of UGT2B7 protein expression in HuH-7 cells transfected with 100 nM of scrambled or miR-216b-5p inhibitor. Panel *F*; UGT2B7 glucuronidation activity against epirubicin in HuH-7 cells transfected with 100 nM of scrambled or miR-216b-5p inhibitor. Panel *G*; Representative blot of UGT2B7 protein expression in Hep3B cells transfected with 100 nM of scrambled or miR-216b-5p

Downloaded from jpet.aspetjournals.org at ASPET Journals on April 19, 2024

JPET Fast Forward. Published on July 29, 2016 as DOI: 10.1124/jpet.116.235044
This article has not been copyedited and formatted. The final version may differ from this version.

inhibitor. Panel *H*, bottom; UGT2B7 glucuronidation activity against epirubicin in Hep3B cells transfected with 100 nM scrambled or miR-216b-5p inhibitor. Panel *I,* UGT2B4 glucuronidation activity against codeine in HuH-7 transfected with 250 nM scrambled miRNA mimic or 50 nM, 125 nM, or 250 nM miR-216b-5p mimic. Panel *J*, UGT2B4 glucuronidation activity against codeine in Hep3B cells transfected with 50 nM scrambled miRNA mimic or 10 nM, 25 nM, or 50 nM miR-216 mimic. Panel *K,* UGT2B10 glucuronidation activity against nicotine in HuH-7 cells transfected with 100 nM scrambled miRNA mimic or 10 nM, 50 nM, or 100 nM miR-216b-5p mimic. Panel *L*, UGT2B10 glucuronidation activity against nicotine in Hep3B cells transfected with 50 nM scrambled or miR-216b-5p mimic. Columns represent the mean ± S.E. of three independent experiments. * $P<0.05$; ** $P<0.01$, *** $P<0.001$.

Downloaded from jpet.aspetjournals.org at ASPET Journals on April 19, 2024

Table 1. List of PCR primers used for UGT2B 3′ UTR PCR amplification, cloning, and luciferase mutational analysis.

Primer	Sequence
Outer UGT2B7 3′ UTR For	5’ – CCTTCGGGTTGCAGCCCACGAC – 3’
Outer UGT2B7 3’ UTR Rev	5’ – ATAGGCTCTCAGGATTCAGAGGGGAGGG – 3’
Inner UGT2B7 3’ UTR For	5’ – GCTATCTAGAGTTATATCTGAGATTTGAAGCTGGAAAACC – 3’
Inner UGT2B7 3’ UTR Rev	5’ – GCTATCTAGATAAGGCTTTATCTTATTTTTTATTTTCCG – 3’
UGT2B4 3’ UTR For	5’ – GCTATCTAGATTACGTCTGAGGCTGGAAGCTG – 3’
UGT2B4 3’ UTR Rev	5’ – GCTATCTAGACACAATCCTGCATGAAATGATCC – 3’
UGT2B10 3’ UTR For	5’ – GCTATCTAGAGGGATTAGTTATATCTGAGATTTGAAGCTGG – 3’
UGT2B10 3’ UTR Rev	5’ – GCTATCTAGACCTAAGTCATCATGACCATGGCTCAGAGTG – 3’
UGT2B7 216b Del. SDM For	5’ – CCTTGTCAAATAAAAATTTGTTTTTCAGTTACCACCCAGTTCATGGTT – 3’
UGT2B7 216b Del. SDM Rev	5’ – TAACCATGAACTGGGTGGTAACTGAAAAACAAATTTTTATTTGACAAAG – 3’
UGT2B4 216b Del. SDM For	5’ – TTATTACAACAATAAGACGTTGTGATACAATTCCTTTCTTCTTGTG – 3’
UGT2B4 216b Del. SDM Rev	5’ – CACAAGAAGAAAGGAATTGTATCACAACGTCTTCTTGTTGTAATAA – 3’
UGT2B10 216b Del. SDM For	5’ – CTACCTTGTCAAGTAAAATTTGTTTTTCATTTACCACCCAGTTAATG – 3’
UGT2B10 216b Del. SDM Rev	5’ – CCATTAACTGGGTGGTAAATGAAAAACAAATTTTTACTTGACAAGGTAG – 3’
UGT2B10 SNP rs139538767 SDM For	5’ – CAAGTAAAAATTTGTTTTTCAGAGGTTTACCACCCAGTTAATGGTTAG – 3’
UGT2B10 SNP rs139538767 SDM Rev	5’ – CTAACCATTAACTGGGTGGTAAACCTCTGAAAAACAAATTTTTACTTG – 3’
miR-216b-5p	5’ – AAATCTCTGCAGGCAAATGTGA – 3’

SDM, site-directed mutagenesis; Del, deletion; For, forward; Rev, reverse; SNP, single nucleotide polymorphism

Downloaded from jpet.aspetjournals.org at ASPET Journals on April 3, 2024

Figure 1

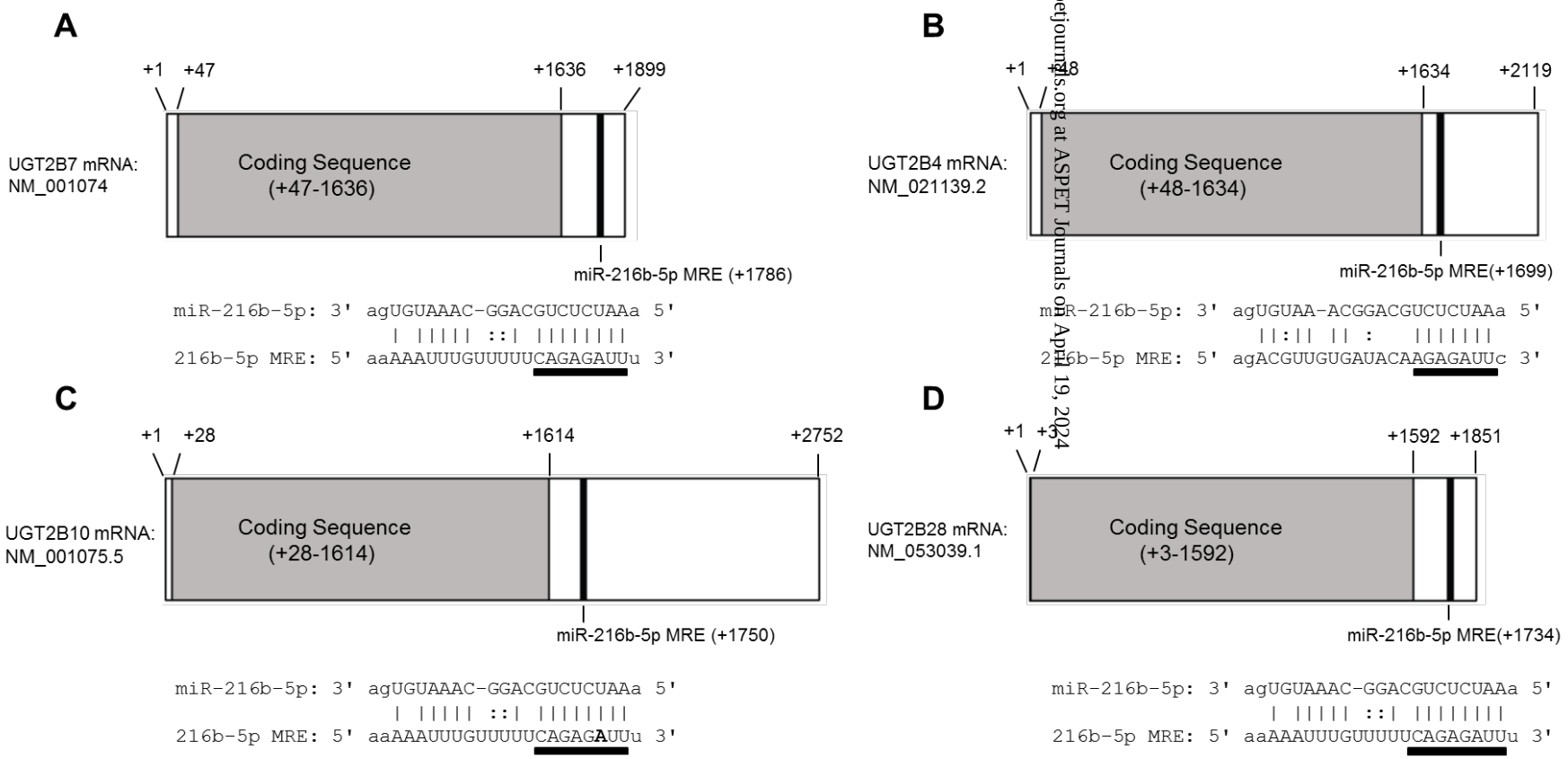

Downloaded from jpet.aspetjournals.org at ASPET Journals on April 19, 2024

Figure 2

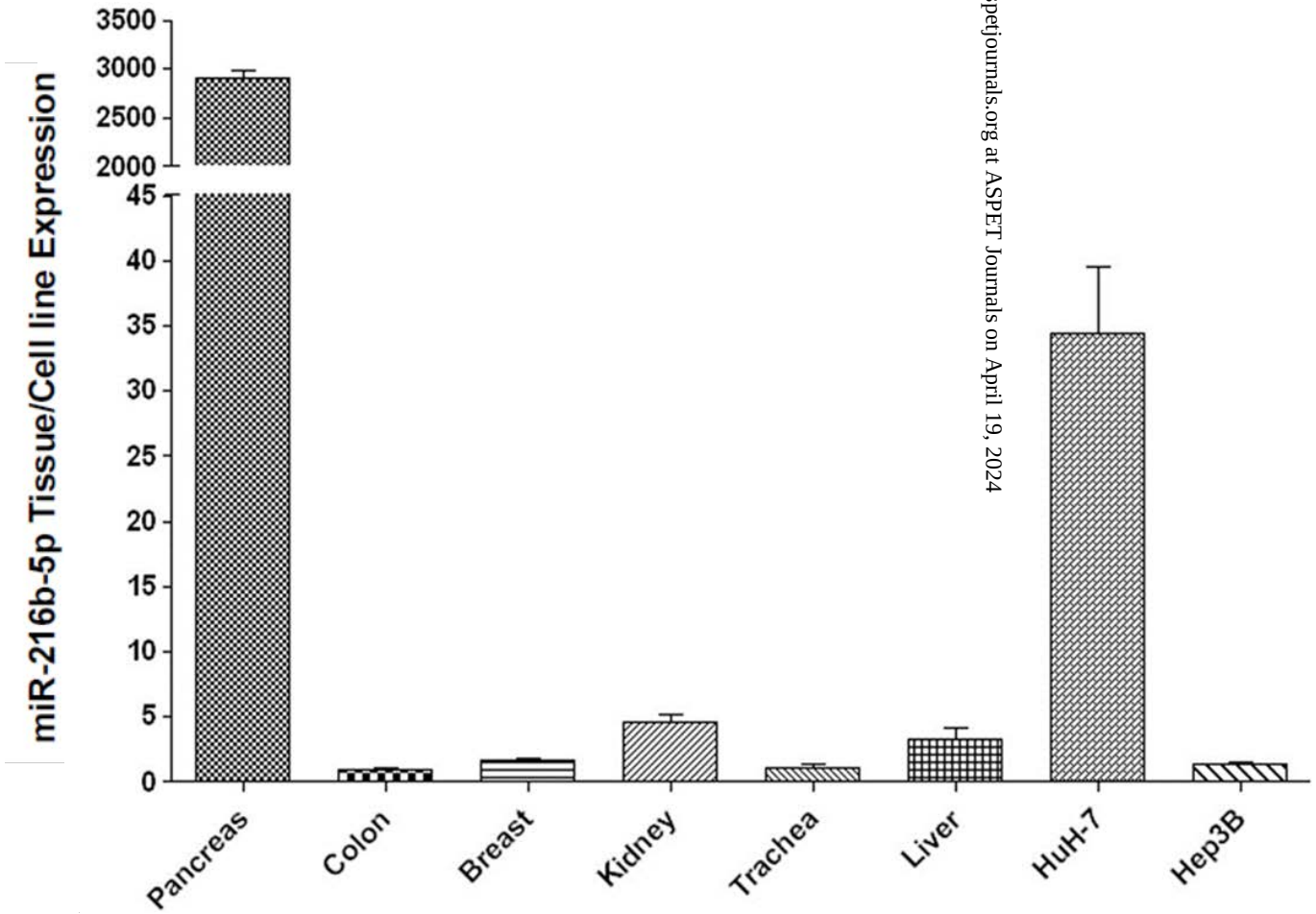

Ct mean:	23.1	31.0	30.8	30.3	32.2	31.2	26.6	30.7

Downloaded from jpet.aspetjournals.org at ASPET Journals on April 19, 2024

JPET Fast Forward. Published on July 29, 2016 as DOI: 10.1124/jpet.116.235044
This article has not been copyedited and formatted. The final version may differ from this version.

Figure 3

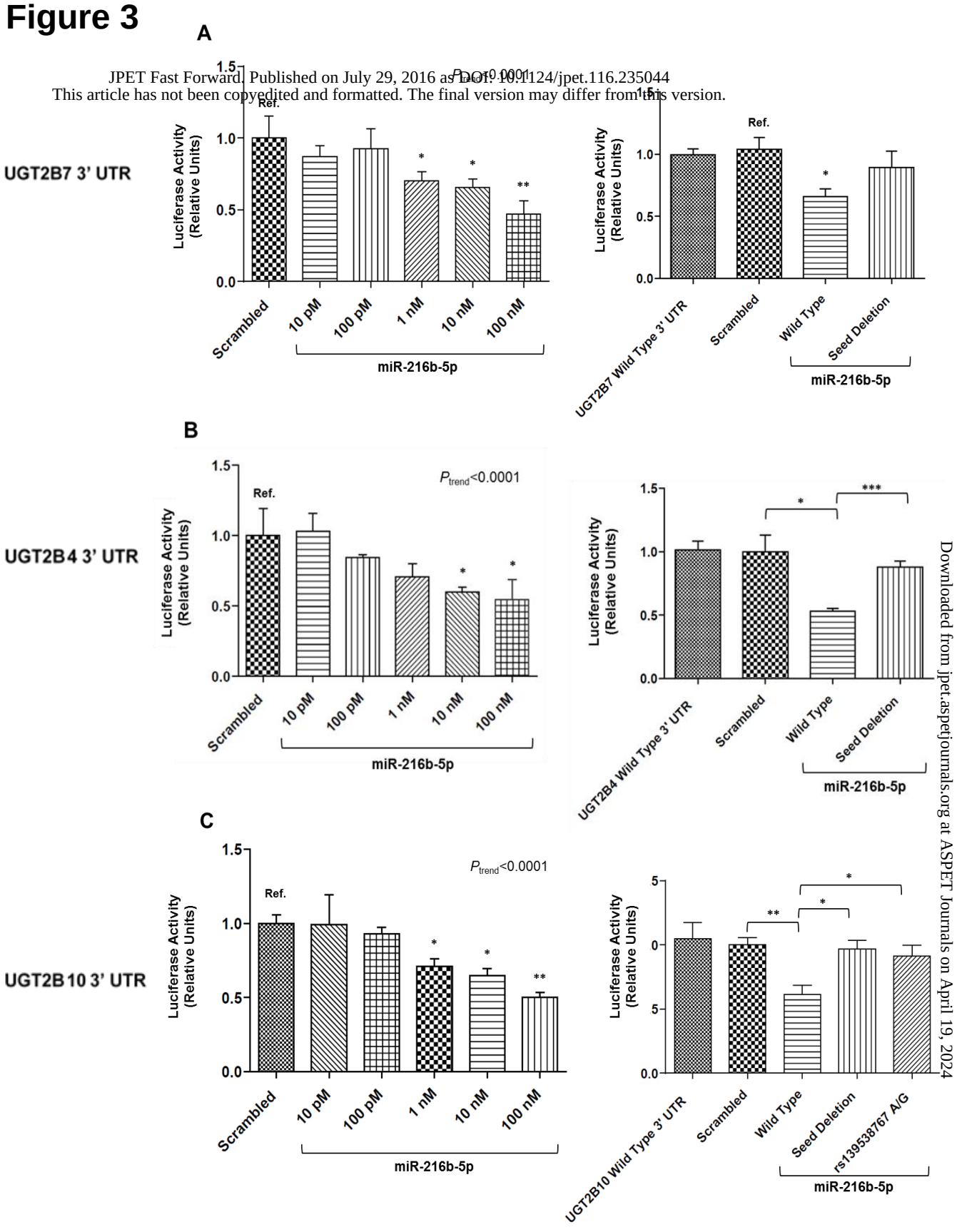

Downloaded from jpet.aspetjournals.org at ASPET Journals on April 19, 2024

Figure 4

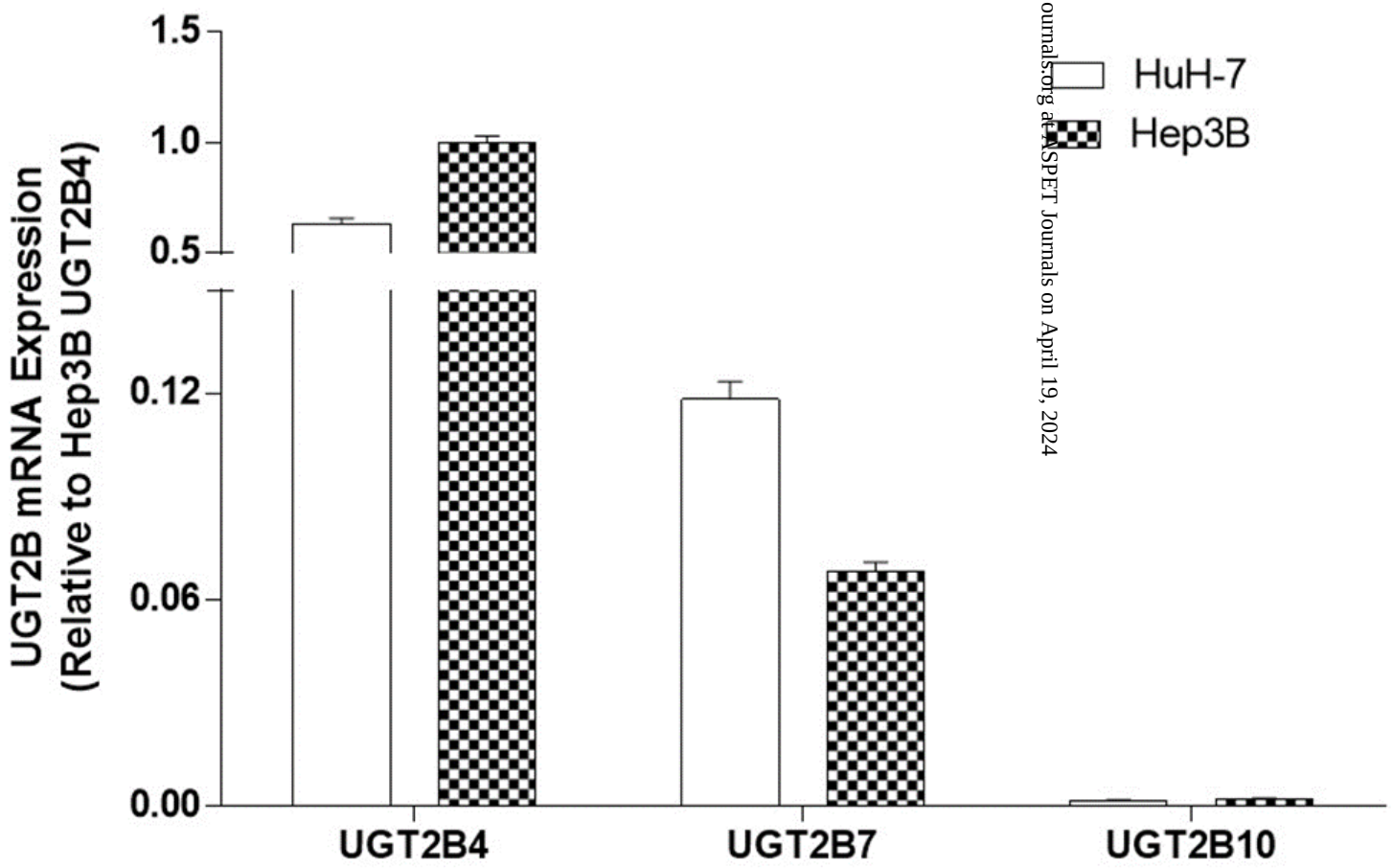

Downloaded from jpet.aspetjournals.org at ASPET Journals on April 19, 2024

Figure 5

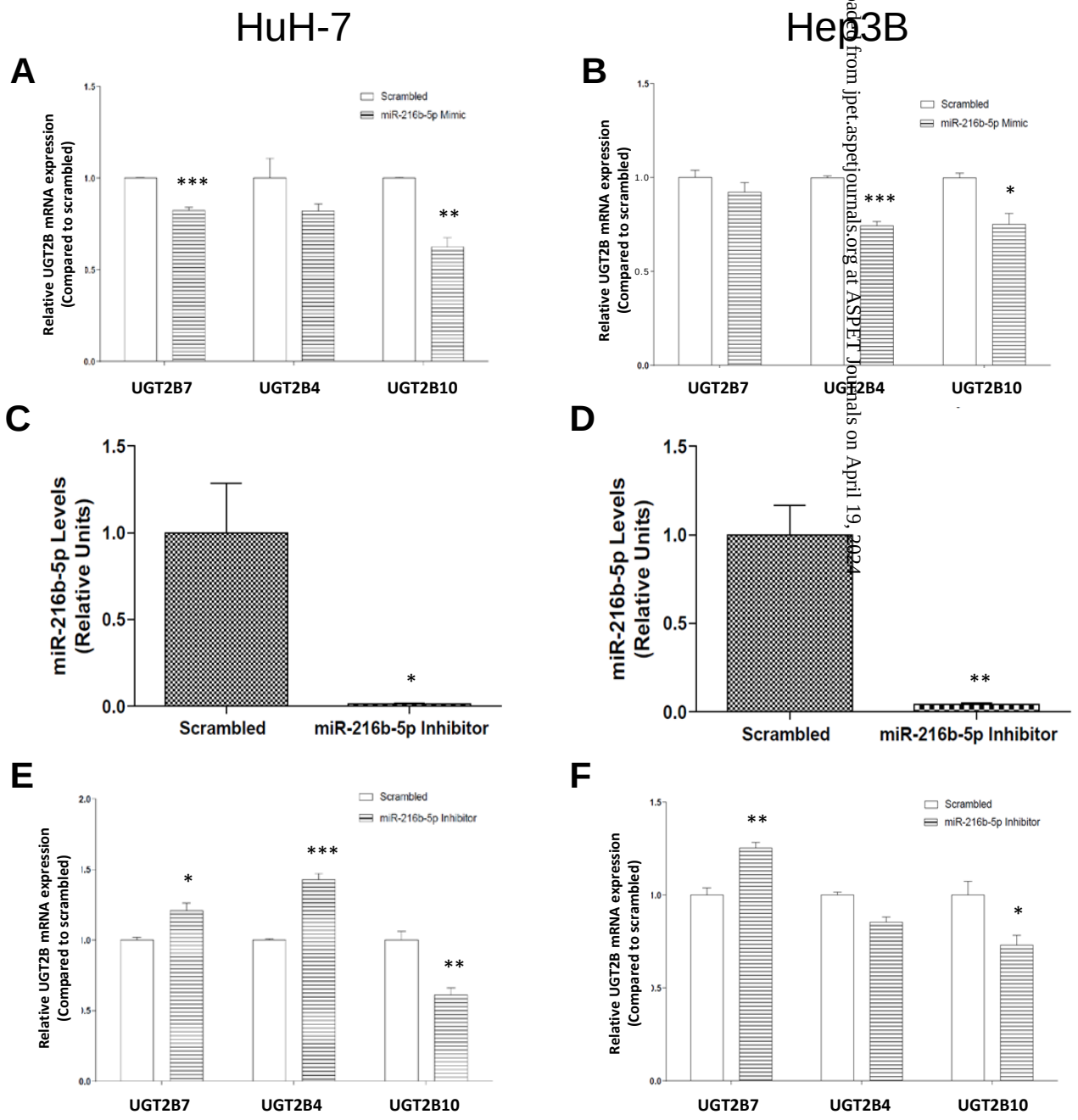

Downloaded from jpet.aspetjournals.org at ASPET Journals on April 19, 2024

Figure 6

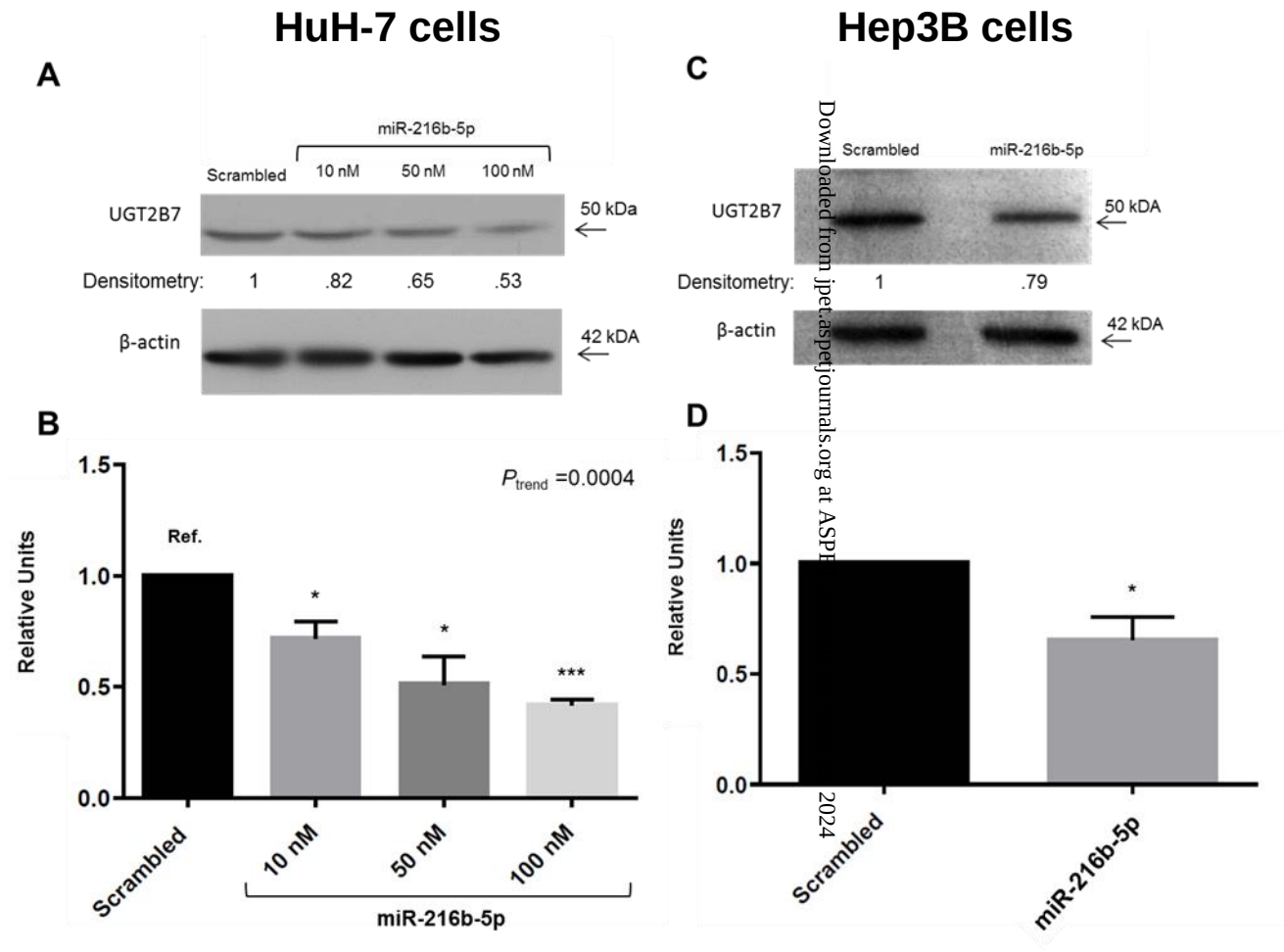

Downloaded from jpet.aspetjournals.org at ASPE
2024

glucuronidation activity against epirubicin

Figure 6

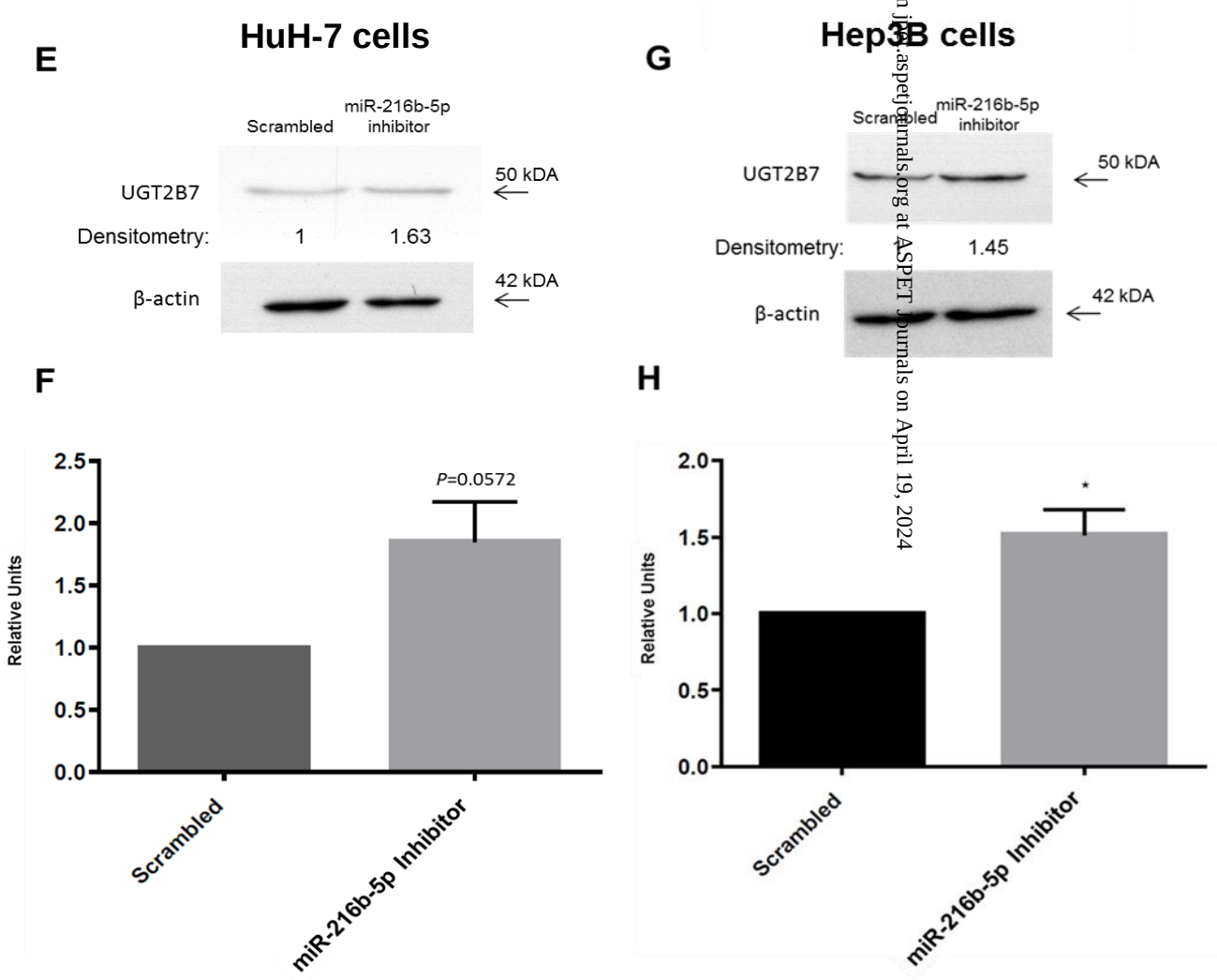

glucuronidation activity against epirubicin

Downloaded from jpet.aspetjournals.org at ASPET Journals on April 19, 2024

Figure 6

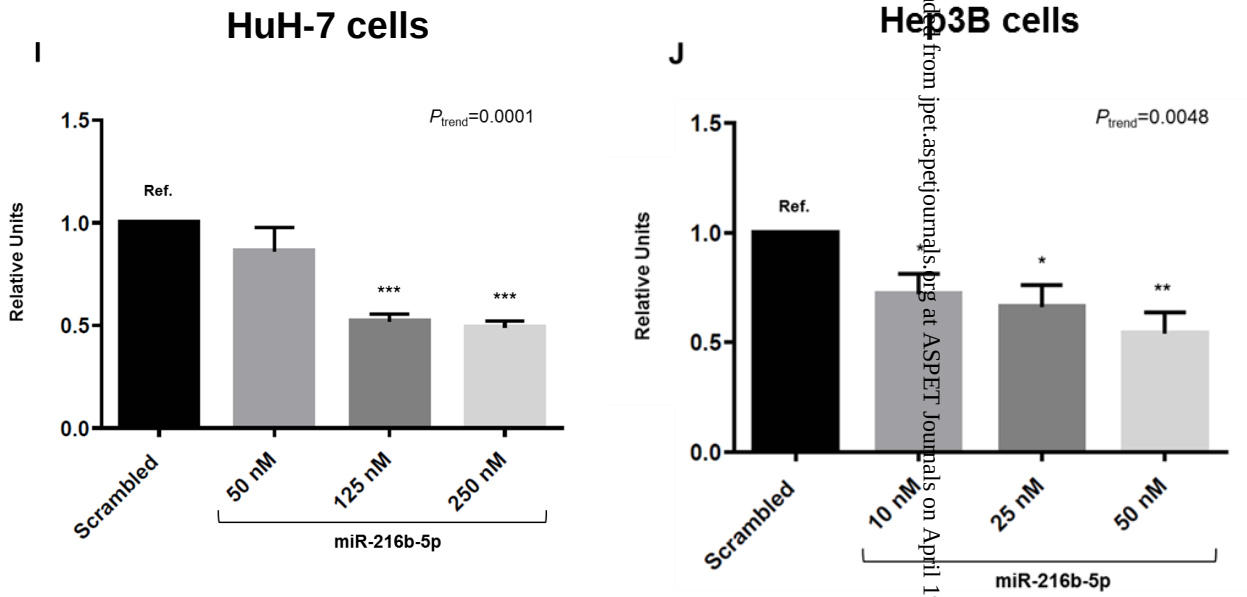

glucuronidation activity against codeine

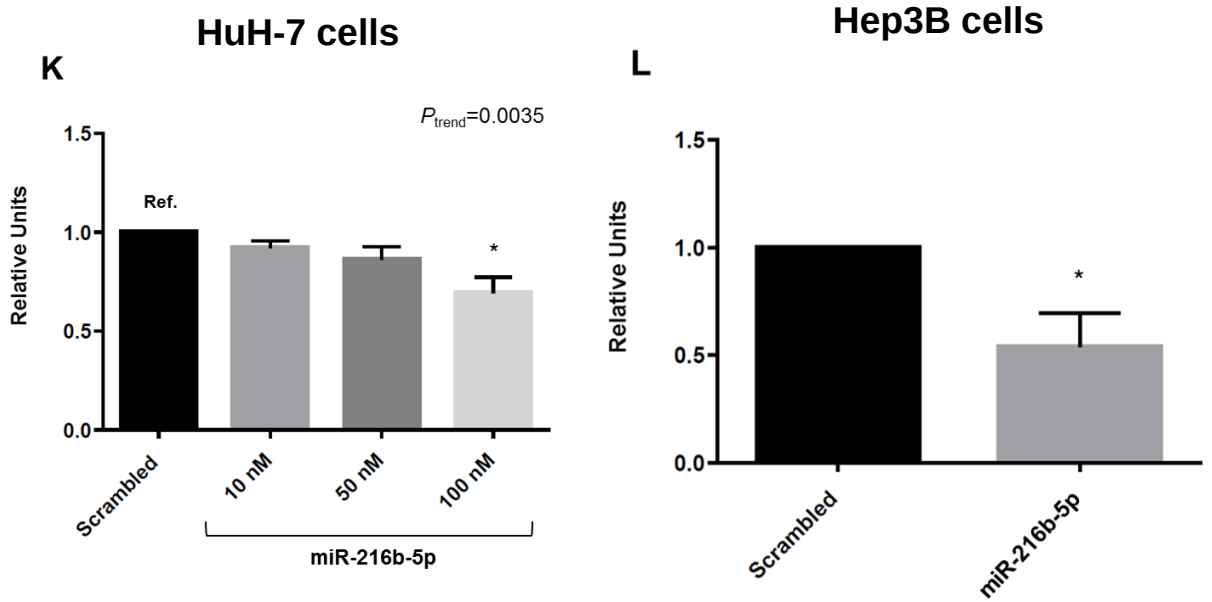

glucuronidation activity against nicotine

Downloaded from jpet.aspetjournals.org at ASPET Journals on April 19, 2024